THE JOURNAL OF COMPARATIVE NEUROLOGY 481:160–178 (2005)

Organization of Hypocretin/Orexin Efferents to Locus Coeruleus and Basal Forebrain Arousal-Related Structures

RODRIGO A. ESPAÑA,[1] KATE M. REIS,[1] RITA J. VALENTINO,[2] AND CRAIG W. BERRIDGE[1]*
[1]Department of Psychology, University of Wisconsin, Madison, Wisconsin 53706-1611
[2]Children's Hospital of Philadelphia, Philadelphia, Pennsylvania 19104

ABSTRACT

Hypocretin/orexin neurons give rise to an extensive projection system, portions of which innervate multiple regions associated with the regulation of behavioral state. These regions include the locus coeruleus, medial septal area, medial preoptic area, and substantia innominata. Evidence indicates that hypocretin modulates behavioral state via actions within each of these terminal fields. To understand better the circuitry underlying hypocretin-dependent modulation of behavioral state, the present study characterized the degree to which there exists: 1) lateralization of hypocretin efferents to basal forebrain and brainstem arousal-related regions, 2) topographic organization of basal forebrain- and brainstem-projecting hypocretin neurons, and 3) collateralization of individual hypocretin neurons to these arousal-related terminal fields. These studies utilized combined immunohistochemical identification of hypocretin neurons with single or double retrograde tracing from the locus coeruleus, medial preoptic area, medial septal area, and substantia innominata. Results indicate that approximately 80% of hypocretin efferents to basal forebrain regions project ipsilaterally, whereas projections to the locus coeruleus are more bilateral (65%). There was a slight preference for basal forebrain-projecting hypocretin neurons to be distributed within the medial half of the hypocretin cell group. In contrast, hypocretin neurons projecting to the locus coeruleus were located primarily within the dorsal half of the hypocretin cell group. Finally, a large proportion of hypocretin neurons appear to project simultaneously to at least two of the examined terminal fields. These latter observations suggest coordinated actions of hypocretin across multiple arousal-related regions. J. Comp. Neurol. 481:160–178, 2005.

Indexing terms: medial preoptic area; medial septum; lateral hypothalamus; retrograde tract tracing; substantia innominata; orexin; locus coeruleus

The hypocretin (HCRT) system has been implicated in the regulation of behavioral state and state-dependent processes. For example, intracerebroventricular (ICV) administration of HCRT-1 and HCRT-2 elicits a robust increase in time spent awake. HCRT-induced waking is accompanied by a variety of behaviors typically observed during spontaneous waking and/or under stressful, high-arousal conditions, depending on dose and testing conditions (Hagan et al., 1999; Ida et al., 1999; Piper et al., 2000; España et al., 2001, 2002, 2003). Consistent with the posited role of HCRT in waking/arousal, dysregulation of HCRT neurotransmission appears to underlie symptoms associated with narcolepsy (Chemelli et al., 1999; Lin et al., 1999; Nishino et al., 2000; Thannickal et al., 2000).

HCRT is synthesized in a relatively small population of neurons restricted to the perifornical region of the lateral hypothalamus (Peyron et al., 1998; Sakurai et al., 1998; Date et al., 1999). Nonetheless, HCRT-containing fibers

Grant sponsor: The University of Wisconsin Graduate School (to C.W.B.); Grant sponsor: Public Health Service; Grant number: DA10681; Grant number: DA00389; Grant number: MH62359 (to C.W.B.); Grant number: MH02006; Grant number: MH40008 (to R.J.V.).

*Correspondence to: Craig W. Berridge, Psychology Department, University of Wisconsin, 1202 W. Johnson St., Madison, WI 53706-1611. E-mail: berridge@wisc.edu

Received 27 May 2004; Revised 22 July 2004; Accepted 28 August 2004
DOI 10.1002/cne.20369
Published online in Wiley InterScience (www.interscience.wiley.com).

and receptors are found widely throughout the brain, including within a variety of basal forebrain and brainstem regions associated with the regulation of behavioral state (Peyron et al., 1998; Sakurai et al., 1998; Date et al., 1999; Nambu et al., 1999; Taheri et al., 1999; Bourgin et al., 2000; Greco and Shiromani, 2001; Marcus et al., 2001; España et al., 2001; Hervieu et al., 2001; Backberg et al., 2002; Cluderay et al., 2002; Suzuki et al., 2002). These regions include the locus coeruleus (LC), the general region of the medial preoptic area (MPOA), the general region of the medial septal area (MS), and the substantia innominata (SI). Infusion of HCRT into each of these regions elicits waking and a variety of waking-related behaviors (España et al., 2001; Bourgin et al., 2000; Thakkar et al., 2001). A critical question raised by these latter observations is the extent to which HCRT release is coordinated across multiple functionally related terminal fields.

Understanding of the organization of HCRT efferents to arousal-related terminal fields is essential for a better understanding of the neurobiology of HCRT-dependent regulation of behavioral state. Surprisingly, relatively little information exists concerning the anatomical organization of HCRT efferents to arousal-related structures. For example, the degree to which HCRT efferents are lateralized and whether HCRT neurons are organized topographically with respect to terminal field is currently not known. A topographic organization of HCRT neurons could suggest differential regulation of subpopulations of HCRT neurons and the differential regulation of HCRT neurotransmission across terminal fields. For the LC-noradrenergic system, it has been observed that subsets of individual neurons project to functionally related structures (e.g., cortical, thalamic, and brainstem somatosensory nuclei; Steindler, 1981; Van Bockstaele et al., 1996; Simpson et al., 1997). This presumably permits an individual LC neuron to influence simultaneously the activity of a functional circuit distributed across multiple levels and involving multiple regions of the neuraxis. Currently, the extent to which individual HCRT neurons collateralize to multiple arousal-related regions, and thus might simultaneously impact multiple terminal fields, is not known.

The current studies utilized single and double retrograde labeling of immunohistochemically identified HCRT neurons to characterize the anatomical organization of HCRT efferents to select basal forebrain and brainstem sites. Retrograde tracing using either wheat germ agglutinin-horseradish peroxidase coupled to gold particles (WGA), cholera toxin β-subunit (CTb) or fluorogold (FG) was combined with immunohistochemical localization of HCRT to identify the distribution of HCRT neurons that project to LC, MS, MPOA, or SI. These studies permitted assessment of the degree to which HCRT efferents to these regions are topographically organized and lateralized. Additionally, triple-labeling procedures were used to examine the extent to which individual HCRT neurons collateralize to multiple arousal-related terminal fields. In these studies, animals received a pair of tracer infusions into different terminal fields (e.g., WGA into LC and FG into a basal forebrain region, or CTb and FG into two different basal forebrain regions). The degree to which HCRT neurons were labeled by both tracers was then examined.

MATERIALS AND METHODS

Animals

Adult male Sprague-Dawley rats (300–400 g; Sasco, Oregon, WI) were housed in pairs for at least 14 days prior to surgery with ad lib access to food and water on an 13:11-hour light:dark cycle (lights on 7:00 AM).

Surgery

All animals were anesthetized with halothane and then placed in a stereotaxic instrument with the incisor bar set at –11.5 mm below ear bar zero. Retrograde tracer infusions were made into LC (–4.0A relative to lambda, 1.3L, –5.9V), MS (–1.0A, 1.6L, –2.8V), MPOA (–1.9A, 1.8L, –3.4V), or SI (–1.9A, 3.1L, –3.7V) using glass pipettes (see below). In all cases, an incision was made in the dura mater with a 30-ga. needle prior to insertion of the infusion pipette. At the end of surgery, all animals received buprenorphine (0.01 mg/kg; Reckett Beckiser Pharmaceutical, Inc., Richmond, VA) and penicillin (300,000 U/ml; G.C. Handford Mfg. Co., Syracuse, NY). All facilities and procedures were in accordance with the guidelines regarding animal use and care put forth by the National Institutes of Health and were supervised and approved by the Institutional Animal Care and Use Committee of the University of Wisconsin

Infusion procedures

WGA infusions into LC. Because of its highly restricted intratissue diffusion, WGA was used as a retrograde tracer to identify HCRT efferents to LC (Van Bockstaele et al., 1998). For these infusions, one barrel of a double-barrel glass micropipette was used to localize LC via extracellular electrophysiological recordings, and the second barrel was used to infuse WGA. Double-barrel pipettes were manufactured as previously described (Valentino et al., 1992). Briefly, these pipettes consisted of a recording pipette (7–10 μm tip diameter; Friedrich and Dimmock Inc., Millville, NJ) cemented with 3M single-bond dental adhesive (Patterson Dental Supply, St. Paul, MN) to a microinfusion pipette (20–50 μm tip diameter; Fisher Scientific, Itasca, IL). The microinfusion pipette was angled at 30–45°, with the tip approximately 100 μm dorsal to the recording pipette tip. The recording pipette was filled with 2% pontamine sky blue in 0.5 M sodium acetate buffer (pH 8.4). The microinfusion pipette was filled with a solution of WGA-horseradish peroxidase (Sigma, St. Louis, MO) coupled to 10-nm gold (gold chloride; Sigma) as previously described (Basbaum and Menetrey, 1987; Drolet et al., 1992). LC neuronal activity was identified based on electrophysiological characteristics as described elsewhere (Valentino et al., 1983). WGA was infused into the LC nucleus or into the rostromedial pericoerulear dendritic zone (Shipley et al., 1996). Infusions of WGA were made as described previously (Valentino et al., 1992, 1996). Briefly, the infusion micropipette was connected via tubing to a source of solenoid-activated pneumatic pressure (Picospritzer; General Valve, Fairfield, NJ), and WGA was ejected by applying small pulses of pressure (40–80 psi, 50–100 msec duration). Pipettes were calibrated such that known amounts of solution could be ejected by measuring displacement of the liquid column (60 nl/mm). For all cases, approximately 150–300 nl of solution was ejected over a period of at least 10 minutes. After injection, the-double barrel micropipette

was kept in position for an additional 10 minutes. Animals were killed 7 days following surgery and infusion.

FG and CTb infusions into basal forebrain regions. FG and CTb were used as retrograde tracers to identify HCRT efferents to MS, MPOA, or SI. For infusions of FG, single-barrel glass micropipettes (5–20 μm diameter; Friedrich and Dimmock) were filled with a 2% FG solution (dissolved in saline) as described previously (Valentino et al., 1994). Once the infusion pipette was in position, FG was iontophoresed (5.0 μA, 15 minutes, 5 second pulses, 50% duty cycle) and the pipette left in place for 10 minutes. For infusions of CTb, single-barrel glass micropipettes (20–30 μm diameter; Friedrich and Dimmock) were filled with 1.0% CTb solution (dissolved in 0.1 M phosphate buffer, pH 6.0) as described previously (Valentino et al., 1994). CTb was ejected by applying small pulses of pressure (40–80 psi, 50–100 msec duration) to the calibrated pipette (60 nl/mm). For all cases, approximately 200–300 nl of solution was ejected over a period of at least 10 minutes, and the pipette was left in place for an additional 10 minutes.

For both FG and CTb, infusion volume was chosen to provide diffusion of tracer throughout a substantial portion of each basal forebrain region identified in previous studies to be sensitive to the wake-promoting actions of HCRT (España et al., 2001; see Figs. 2, 5). For both FG and CTb, animals were sacrificed 7 days following infusion.

To examine collateralization of HCRT efferents to LC and basal forebrain structures, unilateral infusions of both WGA (within LC) and FG (within MS, MPOA, or SI) were made in the same animal. In these cases, infusion of WGA was made prior to FG infusion using the above-described protocols. To examine collateralization of HCRT efferents to basal forebrain structures, an infusion of FG was made into MS, MPOA, or SI, and a CTb infusion was made into one of the two remaining basal forebrain regions in the same animal. In all cases, combinations of retrograde tracer infusions were made into the same hemisphere (e.g., WGA into the left LC and FG into the left MPOA). Animals were killed 7 days following the infusions.

Histology and immunohistochemistry

All animals were deeply anesthetized with pentobarbital (Abbott Laboratories, North Chicago, IL) and perfused transcardially with 250 ml of heparinized saline (1 U heparin/ml 0.9% saline; SoloPak Laboratories, Elk Grove Village, IL), followed by 400 ml of 4.0% paraformaldehyde in 0.01 M phosphate buffer (pH 7.4). Brains were removed, stored in formaldehyde overnight, and taken through graded sucrose solutions (20–30% sucrose in 0.01 M phosphate buffer, pH 7.4). A tracking mark was made in the right lateral cortex and brainstem to identify this hemisphere in tissue sections. Forty-micrometer-thick sections were collected on a cryostat and placed in 0.01 M phosphate-buffered saline (PBS; pH 7.4) with 0.1% sodium azide and stored at 4°C. To examine the degree to which HCRT efferents are lateralized, brain sections were processed to visualize prepro-HCRT and either FG or WGA alone using standard immunoperoxidase procedures. For animals receiving only WGA infusion, sections were first reacted for WGA (silver intensification: black reaction product) and then processed to visualize prepro-HCRT (brown reaction product). For animals receiving only FG infusions, sections were first processed for prepro-HCRT (brown reaction product) and then processed to visualize FG (blue reaction product).

To examine the extent to which individual HCRT neurons send axon collaterals to LC and individual basal forebrain structures, brain sections were processed to visualize prepro-HCRT and both FG and WGA using standard immunoperoxidase procedures. Sections were first processed to visualize WGA, stained for prepro-HCRT (brown reaction product), and then stained for FG (blue reaction product). To examine collateralization of HCRT efferents to basal forebrain structures, brain sections were processed to visualize prepro-HCRT, FG, and CTb by using immunofluorescence techniques. Sections were first stained for prepro-HCRT (red fluorophore using a standard rhodamine fluorescence cube) and then processed to visualize CTb (green fluorophore using a standard fluorescein fluorescence cube). Because FG exhibits autofluorescent properties (observed as a yellow/gold fluorophore with a modified UV fluorescence cube; Chroma Technology Corporation, Brattleboro, VT), no immunofluorescence processing was required for visualization of FG. These staining procedures allowed for optimal microscopic discrimination of single (FG, WGA, or HCRT)-, double (FG + HCRT, WGA + HCRT)-, and triple (FG + WGA + HCRT)-labeled cells and did not appear to alter the staining quality or the average cell counts commonly observed when staining independently for FG, prepro-HCRT, or WGA.

Brightfield microscopy

WGA was visualized by using the IntenSE BL silver enhancement kit (Amersham, Piscataway, NJ) to localize the transported gold-protein conjugate, as described previously (Drolet et al., 1992). Sections were rinsed three times in 0.1 M citrate acetate buffer (pH 5.5) and incubated with the kit enhancer and initiator for 30 minutes in the dark. The sections were then rinsed twice in citrate acetate buffer and reacted for 5 minutes with sodium thiosulfate (2.5% in 0.1 M phosphate buffer, pH 7.4).

For immunoperoxidase processing of prepro-HCRT, sections were rinsed with 0.01 M PBS and incubated for 30 minutes in a quench solution containing 0.75% hydrogen peroxide, rinsed again, and incubated for 48 hours at 4°C with rabbit anti-rat prepro-HCRT antibody (1:2000; Chemicon International, Temecula, CA). The antibody was diluted in 0.01 M PBS containing 0.1% Triton X-100 (PBS-TX). After incubation, tissue was rinsed with 0.01 M PBS, and incubated with biotinylated goat anti-rabbit antisera (1:200; ABC Elite kit; Vector Laboratories, Burlingame, CA) for 90 minutes. After incubation, sections were rinsed with 0.01 M PBS, incubated in avidin-biotin solution (ABC Elite kit) for 90 minutes, rinsed again with 0.01 M PBS, and then reacted with diaminobenzidene (DAB; Vector Laboratories) to yield a brown precipitate.

For immunoperoxidase processing of FG, sections were rinsed with 0.01 M PBS and then incubated for 20 minutes in a quench solution containing 0.75% hydrogen peroxide. Sections were then rinsed and incubated for 48 hours at 4°C with rabbit anti-FG antibody (1:2,000; Chemicon International) diluted in 0.01 M PBS-TX. After incubation, tissue was rinsed with 0.01 M PBS-TX and incubated with donkey anti-rabbit antibody (1:500; Jackson Immunoresearch, West Grove, PA) for 90 minutes. Tissue was then rinsed with 0.01 M PBS-TX, exposed to

rabbit PAP (1:500; Dako Corporation, Carpinteria, CA) for 90 minutes, and rinsed with 0.01 M PBS-TX. Sections were then reacted with SG blue (Vector Laboratories) to yield a blue/gray precipitate. All sections were mounted on microscope slides (Fisher Scientific), air dried, taken through graded alcohols (50–100%), cleared for 24 hours (Histoclear; Fisher Scientific), and coverslipped with DPX mounting medium (BDH Laboratory Supplies, Garden City, NY).

Fluorescent microscopy

For immunofluorescence processing of prepro-HCRT, sections were rinsed with 0.01 M PBS and incubated for 30 minutes in a 5.0% normal goat serum blocking solution, rinsed again, and incubated for 48 hours at 4°C with rabbit anti-rat prepro-HCRT antibody (1:500; Chemicon International). The antibody was diluted in 0.01 M PBS-TX. After incubation, tissue was rinsed with 0.01 M PBS and incubated with biotinylated goat anti-rabbit antisera (1:200; ABC Elite kit) for 90 minutes. After incubation, sections were rinsed with 0.01 M PBS and incubated in a Cy3-conjugated streptavidin (Jackson Immunoresearch) for 60 minutes. For immunofluorescence processing of CTb, sections were rinsed with 0.01 M PBS and then incubated for 3 hours at room temperature with a fluorescein-conjugated rabbit anti-CTb antibody (1:100; Accurate Chemical and Scientific Corporation, Westbury, NY). All sections were mounted on microscope slides (Fisher Scientific), air dried, and coverslipped with Prolong mounting medium (Molecular Probes, Eugene, OR).

Data analyses and photomicrograph production

Cell counts were performed at various rostrocaudal locations within LH with an Olympus BX51 light and reflected immunofluorescence microscope. Single (FG, WGA, or HCRT)-, double (FG + HCRT, WGA + HCRT)-, or triple (FG + WGA + HCRT)-labeled neurons were counted from both hemispheres in four to six sections per animal. Tissue sections utilized in these analyses included at least one rostral, one central, and one caudal HCRT-rich section, separated by approximately 400 μm. Numbers derived from these counts were subsequently averaged for analysis.

In a subset of animals, analyses were conducted to examine the topography of double-labeled neurons in the rostrocaudal dimension. In these analyses, the percentages of double-labeled neurons were compared across the three rostrocaudal levels. Additional analyses were conducted to examine the topography of double-labeled neurons within both mediolateral and dorsoventral dimensions. In these latter analyses, digital images were collected from the densest HCRT-rich section available for each animal (typically located centrally in the rostrocaudal dimension). The HCRT cell group within each of these images was divided into four quadrants, the origin of which was positioned within the center of the HCRT population (Fig. 1). In these analyses, single- and double-labeled neurons were counted from each quadrant. These numbers were then averaged to provide a value for each dorsal, ventral, medial, and lateral quadrant for each animal. It was not feasible to assess topographic distribution of triple-labeled neurons in the dual retrograde tracer studies because of the low absolute numbers of triple-labeled neurons obtained in these studies.

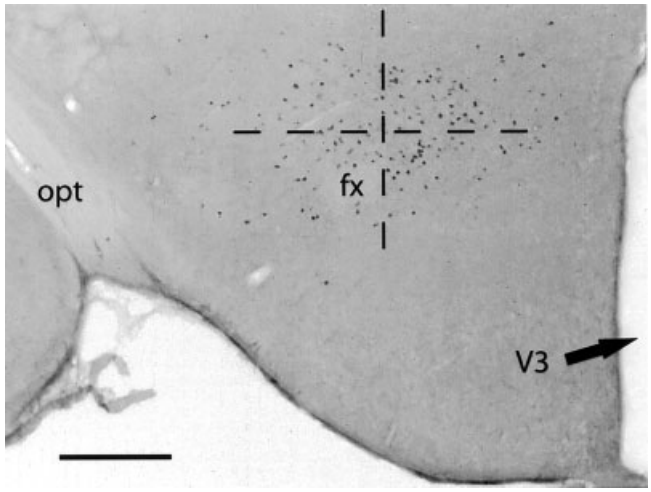

Fig. 1. Photomicrograph depicting the distribution of prepro-HCRT-ir neurons within the lateral hypothalamus. For some analyses, the HCRT group was divided into four equal quadrants, as depicted by the dashed lines (see Materials and Methods). fx, Fornix; opt, optic tract; V3, third ventricle. Scale bar = 500 μm.

Brightfield photomicrographs were acquired with either a Nikon D100 digital camera (black and white images; Nikon Corp.) or an Axiocam MRc digital camera (color images; Carl Zeiss, Inc.) connected to a Zeiss Axioplan light and reflected immunofluorescence microscope. Fluorescent photomicrographs were acquired with a Zeiss LSM 510 UV META upright confocal microscope system. All digital images were matched for brightness and contrast in Adobe Photoshop 6.0 software and labeled in Adobe Illustrator 10.0 software. Figures were printed on a dye-sublimation printer (Kodak XLS 8600PS; Eastman-Kodak).

RESULTS

Retrograde labeling of HCRT neurons from MS, MPOA, and SI

Overview. To examine the extent to which HCRT projections to basal forebrain arousal-related structures are lateralized and topographically organized, the retrograde tracer FG was infused within the general regions of MS, MPOA or SI. For MS and MPOA, previous studies have defined boundaries for the wake-promoting actions of HCRT (España et al., 2001). As determined in these studies, these regions are anatomically heterogeneous, containing a variety of distinct anatomical structures. Thus, the general region defined as MS includes the medial septum, portions of the vertical and horizontal limbs of the nucleus of the diagonal band of Broca (NDB), and the most medial portions of the nucleus accumbens and LPO (see Fig. 3). The general region defined as MPOA contains several preoptic structures, including the medial preoptic area proper (MPO), the medial preoptic nucleus (MPN), and the median preoptic nucleus (see Fig. 6). Given the anatomical resolution of previously conducted microinfusion studies, the precise site(s) of action in the behavioral state modulatory actions of HCRT within MS and MPOA is not known. In contrast to MS and MPOA, SI is a rela-

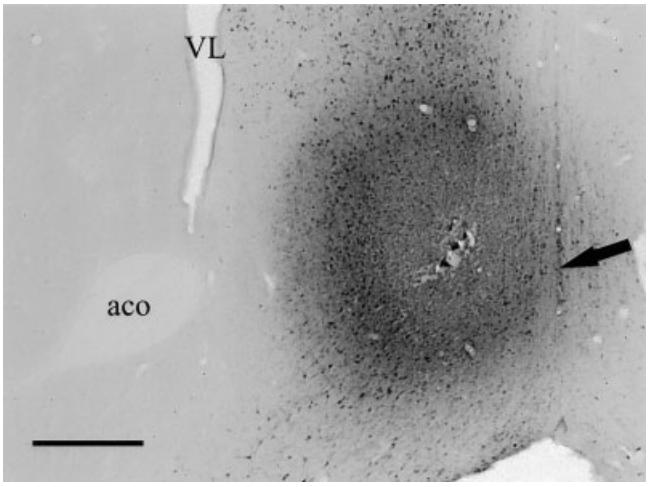

Fig. 2. Photomicrograph depicting a representative FG infusion within MS. Shown is a relatively large FG infusion located largely within the medial septum and the dorsalmost aspects of the vertical limb of the diagonal band of Broca. Note the relatively well-demarcated border of the infusion, with little diffusion into adjacent regions. The arrow points to midline. aco, Anterior commissure; VL, lateral ventricle. Scale bar = 400 μm.

tively homogenous region lacking multiple anatomically defined subnuclei. Nevertheless, an HCRT-responsive region is located within the general region of SI that includes the magnocellular preoptic area as well as the lateral and caudal portions of NDB (see Fig. 9; España et al., 2001). For the majority of cases, retrograde tracer infusions were made to fill a substantial portion of a given HCRT-sensitive region as defined in these previous sleep-wake studies. FG and prepro-HCRT-ir neurons were identified by using immunoperoxidase techniques.

MS. FG infusions were made into MS in 14 animals. In the majority of cases, FG infusions largely targeted the medial septum and the vertical limb of the NDB (Figs. 2, 3). In four animals, FG infusions were located slightly ventral to the medial septum, within the dorsal-most aspect of the NDB horizontal limb. In one animal, the FG infusion was placed immediately medial to the anterior commissure, encompassing portions of the nucleus accumbens (shell and core) and the lateral preoptic area (LPO). In two cases a small amount of FG appeared to cross midline, and in two cases the FG infusions were largely bilateral.

FG infusions into MS resulted in retrograde labeling throughout the posterior hypothalamic region, with particularly dense concentrations of labeled neurons located within the ventral portions of the lateral hypothalamic and perifornical regions. In cases in which the FG infusion was largely unilateral, retrograde labeling was observed primarily ipsilaterally, whereas, in cases in which FG was infused bilaterally, retrograde labeling was also observed bilaterally. A similar pattern of retrograde labeling was observed with infusions into dorsal and ventral portions of MS. In the one case in which FG infusion was made into the nucleus accumbens (shell and core), little labeling was observed within the perifornical region of LH.

Double-labeling immunohistochemistry (FG + HCRT) was conducted with a subset of animals (n = 10) with medium-sized to large (600–1,000 μm diameter) unilateral FG infusions in MS (see Figs. 2, 3). For these cases, the percentage of prepro-HCRT-ir neurons retrogradely labeled with FG was calculated for each hemisphere. These analyses indicated that 9.3% ± 0.7% of prepro-HCRT-ir neurons were labeled ipsilateral to the infusion (Table 1). In contrast, only 2.2% ± 0.2% of prepro-HCRT-ir neurons were labeled contralaterally (Table 1). Thus, of the total prepro-HCRT-ir neurons retrogradely labeled following MS FG infusions (ipsilateral + contralateral), approximately 80% were located ipsilateral to the infusion. Examples of prepro-HCRT-ir neurons retrogradely labeled from MS are shown in Figure 4A,B.

Results obtained from topographic analyses conducted on a subset of animals (n = 5) indicated no major difference in the distribution across medial and lateral aspects of the HCRT-ir field. However, there did appear to be a trend for preferential distribution of retrograde label within the medial half of the HCRT-ir cell group (58% ± 1.1% medial vs. 42% ± 3.0% lateral). No differences in the distribution of retrogradely labeled HCRT neurons were observed dorsoventrally or rostrocaudally.

MPOA. FG infusions were made into the general region defined as MPOA in eight cases. In three of these, FG infusions were confined to the ventromedial portion of MPOA encompassing entirely the medial preoptic nucleus and the majority of MPO (Figs. 5, 6). In three cases, infusions were placed more dorsally, immediately ventral to the anterior commissure. Additionally, in two animals, infusions were located lateral to the medial preoptic nucleus and encompassed the majority of the MPO and a small portion of the LPO.

Retrograde labeling was observed throughout the posterior hypothalamic region, with particularly dense concentrations of labeled neurons located within the ventral portions of the lateral hypothalamic and perifornical regions. In all cases, retrograde labeling was observed primarily ipsilaterally. Double-label immunohistochemistry was conducted on a subset of animals in which FG infusions were of moderate to large size (n = 5; see Figs. 5, 6). Ipsilateral to the infusion, 6.8% ± 0.6% of prepro-HCRT-ir neurons were labeled, whereas 1.2% ± 0.2% prepro-HCRT-ir neurons were labeled contralaterally (Table 1). Thus, of the total of prepro-HCRT-ir neurons retrogradely labeled following MPOA FG infusions (ipsilateral + contralateral), approximately 80% were located ipsilaterally. Examples of prepro-HCRT-ir neurons retrogradely labeled from MPOA are shown in Figure 7A,C. Similarly to the case observed with MS, topographic analyses conducted on a subset of animals (n = 4), indicated no major difference in the pattern of distribution of FG across the medial and lateral aspects of the HCRT-ir cell group. Nevertheless, there might exist a slight preferential distribution of retrogradely labeled neurons medially within the HCRT-ir cell group (60% ± 1.1% medial vs. 40% ± 1.0% lateral). No differences in the distribution of retrogradely labeled HCRT neurons were observed dorsoventrally or rostrocaudally.

The ventrolateral preoptic area (VLPO) plays a critical role in the regulation of behavioral state (Sherin et al., 1996; Lu et al., 2000, 2002). Given the close proximity of our MPOA infusions to the VLPO, we examined the degree to which encroachment upon VLPO might have influenced the pattern of retrograde labeling within HCRT-ir neurons. In five of eight animals receiving FG

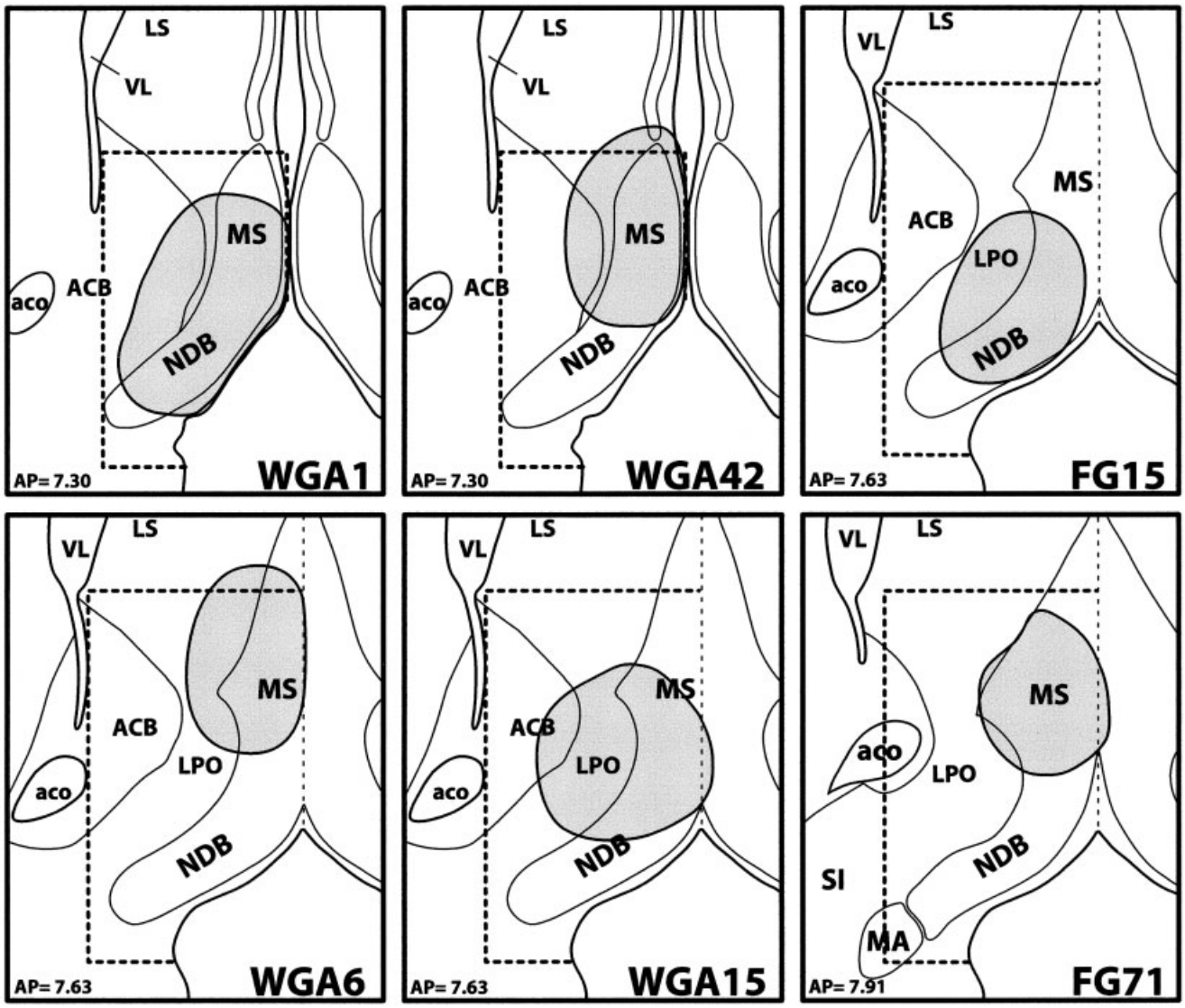

Fig. 3. Schematic depiction of approximate location of FG infusions within MS. Shown are representative infusion locations within MS in six rats. The dashed lines denote the general area demonstrated previously as responsive to the wake-promoting actions of HCRT (España et al., 2001). ACB, nucleus accumbens; aco, anterior commissure; LPO, lateral preoptic area; LS, lateral septum; MA, magnocellular preoptic area; MS, medial septum; NDB, nucleus of the diagonal band of Broca; SI, substantia innominata; VL, lateral ventricle. Adapted from Swanson (1998).

TABLE 1. Mean Number and Percentage of HCRT Neurons Retrogradely Labeled from the Basal Forebrain or from the Locus Coeruleus[1]

	Ipsilateral		Contralateral	
	Mean	Percentage	Mean	Percentage
MS (FG + HCRT)	11.0 ± 0.9	9.3 ± 0.7	2.7 ± 0.3	2.2 ± 0.2
MPOA (FG + HCRT)	8.1 ± 0.7	6.8 ± 0.6	1.7 ± 0.3	1.2 ± 0.2
SI (FG + HCRT)	8.3 ± 0.7	6.8 ± 0.4	2.9 ± 0.4	2.1 ± 0.2
LC (WGA + HCRT)	10.9 ± 0.7	10.9 ± 1.3	5.8 ± 0.5	6.0 ± 1.5

[1]Mean (±SEM) number and percentage (±SEM) of HCRT-ir neurons that were retrogradely labeled from select basal forebrain regions (MS, MPOA, or SI) with FG (FG + HCRT) or retrogradely labeled from LC with WGA (WGA + HCRT).

infusions into MPOA, FG did not encroach substantially upon VLPO. In the remaining three animals, FG infusions appeared to diffuse into VLPO or the extended VLPO to varying degrees. Across these two groups, nearly identical levels of FG labeling of HCRT-ir neurons were obtained (data not shown).

SI. FG infusions were made into the general region of SI in nine animals. In seven of these cases, infusions were largely confined to SI (rostral Ch 4; Mesulam et al., 1983) directly ventral to the anterior commissure and slightly rostral to the level of the decussation of the anterior commissure (Figs. 8, 9). In two animals, FG infusions were located more ventrally and encompassed the ventral aspects of SI and portions of the posterior horizontal limb of the diagonal band of Broca and the magnocellular preoptic nucleus.

As in MS and MPOA, retrograde labeling was observed primarily ipsilaterally throughout LH and adjacent re-

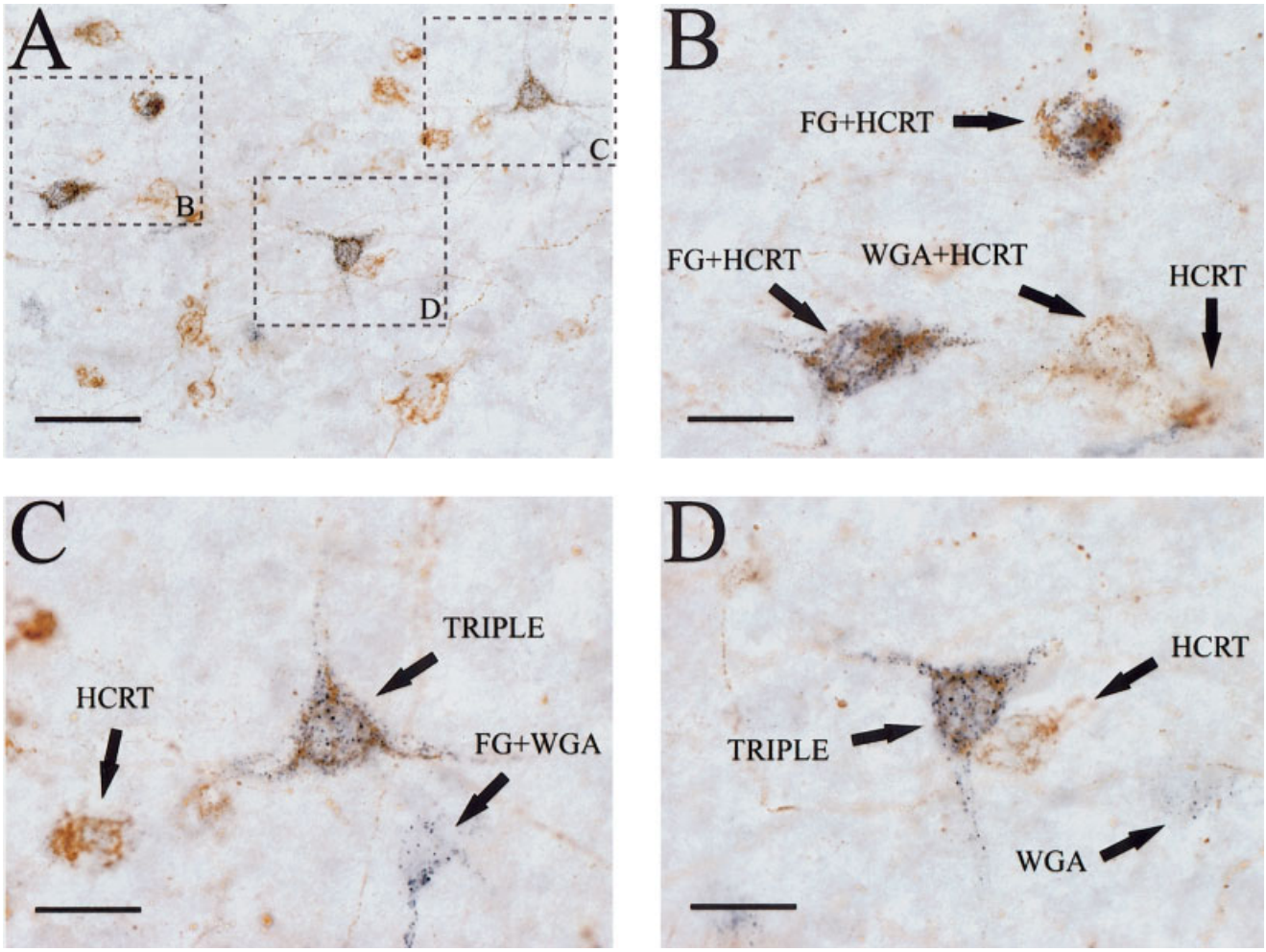

Fig. 4. Photomicrographs depicting retrogradely labeled and prepro-HCRT-ir neurons from one rat infused with FG in MS and with WGA in LC. Shown are FG-labeled (FG; blue), prepro-HCRT-ir (HCRT; brown), and WGA-labeled (WGA; black granules) neurons within the perifornical region of the lateral hypothalamus. Boxes with corresponding letters in A indicate neurons displayed at higher magnification in B–D. **A:** Photomicrograph depicting individual HCRT neurons that project to MS (FG + HCRT), LC (WGA + HCRT), or both MS and LC (triple) as well as non-HCRT neurons that project to MS (FG), LC (WGA), or both MS and LC (FG + WGA). **B–D:** Photomicrographs of the same section as in A. Scale bars = 50 μm in A; 20 μm in B–D.

gions. No obvious differences in retrograde labeling were observed between infusions contained within SI or those placed more ventrally. Double-label immunohistochemistry was conducted on a subset of animals that received medium-sized to large FG infusions (n = 7; see Figs. 8, 9). Ipsilateral to the infusion, 6.8% ± 0.4% of prepro-HCRT-ir neurons were labeled, whereas 2.1% ± 0.2% prepro-HCRT-ir neurons were labeled contralaterally (Table 1). Thus, of the total of prepro-HCRT-ir neurons retrogradely labeled following SI FG infusions (ipsilateral + contralateral), approximately 76% were located ipsilaterally. Examples of prepro-HCRT-ir neurons that were retrogradely labeled from SI are shown in Figure 10A,B. Topographic analyses conducted on a subset of animals (n = 4) suggested a preferential distribution of HCRT neurons retrogradely labeled from SI within the dorsal half of the HCRT-ir cell group (60% ± 3.2% dorsal vs. 40% ± 1.0% ventral). Additionally, similar to the distribution observed with MS and MPOA, no major difference in the distribution of retrograde tracer was observed across medial and lateral aspects of the HCRT-ir cell group (55% ± 1.7% medial vs. 45% ± 2.5% lateral). No difference in rostrocaudal topography was observed.

Retrograde labeling of HCRT neurons from the LC and adjacent regions

To characterize the organization of HCRT efferent projections to LC, WGA infusions were made into the LC nucleus and adjacent dendritic fields in 15 rats (Figs. 11, 12). WGA was identified by using silver intensification, and prepro-HCRT-ir neurons were identified by using immunoperoxidase techniques. WGA infusions into the LC nucleus filled approximately one-fourth to three-fourths of LC and did not extend appreciably outside of the nucleus. Six of these infusions were centered in the dorsal half, three were centered in the ventral half, and six were placed in the center (dorsoventrally) of LC. Of infusions placed in the center of LC, all but one (located within the

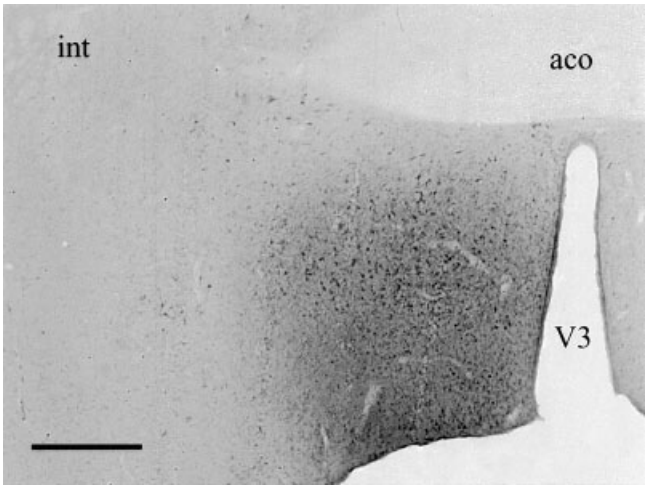

Fig. 5. Photomicrograph depicting a representative FG infusion within MPOA. Shown is a relatively large FG infusion within the medial aspects of MPOA that abuts the third ventricle. Note the relatively well-demarcated border of the infusion with little diffusion into adjacent regions. aco, Anterior commissure; int, internal capsule; V3, third ventricle. Scale bar = 400 μm.

anterior LC; WGA 44) were generally centered rostrocaudally within the main body of LC. In four cases, some WGA was observed medial to LC proper, within the periventricular region. In one case, WGA extended dorsally beyond LC but did not extend into the parabrachial region. As depicted in Figure 13, an additional six rats received WGA infusions within regions adjacent to LC. Five infusions were placed ventral or ventromedial to LC, three of which were within the rostromedial pericoerulear dendritic zone (see Shipley et al., 1996) and two of which within Barrington's nucleus. Additionally, one infusion was placed dorsolateral to LC within the parabrachial nucleus.

Table 1 shows the mean number and percentage of HCRT-ir neurons retrogradely labeled from LC. In the cases in which infusions were placed within LC (Figs. 11, 12), WGA retrograde labeling was observed bilaterally throughout LH and adjacent regions, although the highest concentration of WGA retrograde labeling was observed ipsilaterally (at a ratio of approximately 2:1). Double-label immunohistochemistry demonstrated that, ipsilateral to the WGA infusion, approximately 10.9% ± 1.3% of prepro-HCRT-ir neurons were labeled with WGA. Contralateral to the infusion, 6.0% ± 1.5% prepro-HCRT-ir neurons were labeled (Table 1). Thus, of the total of prepro-HCRT-ir neurons retrogradely labeled with WGA following infusions into LC (ipsilateral + contralateral), approximately 65% were located ipsilateral to the infusion. Examples of prepro-HCRT-ir neurons that were retrogradely labeled from LC are shown in Figures 4B and 7B. Topographic analyses conducted on a subset of animals (n = 9) suggested a stronger topographic organization of HCRT efferents to LC than was observed with basal forebrain terminal fields. Thus, HCRT neurons retrogradely labeled from LC appeared preferentially distributed within the dorsal half of the HCRT-ir cell group (65% ± 2.0% dorsal vs. 35% ± 1.1% ventral). Similarly to the case in the basal forebrain, there was no major difference in the distribution of retrograde label observed across medial and lateral aspects HCRT-ir cell group following WGA infusions into LC (55% ± 1.3% medial vs. 45% ± 1.8% lateral). No difference in rostrocaudal topography was observed. Additionally, tracer placement within LC (mediolaterally, dorsoventrally, or rostrocaudally) did not result in obvious differences in the pattern of labeling of HCRT neurons.

The rostromedial pericoerulear dendritic zone comprises a dense plexus of dopamine β-hydroxylase-positive dendrites extending beyond the boundaries of the LC nucleus (Shipley et al., 1996). In contrast to the LC nucleus, this pericoerulear zone is a target for afferent input from a diversity of regions (Pickel et al., 1977; Arnsten and Goldman-Rakic, 1984; Van Bockstaele et al., 1996, 1998, 1999a, b; Peyron et al., 1998). As such, this pericoerulear zone is considered a critical site for afferent regulation of LC. To examine the degree to which HCRT neurons target this LC dendritic field, WGA was infused into the rostromedial pericoerulear dendritic zone in three animals (Fig. 13; WGA 6, 7, and 48). Double-labeling immunohistochemistry conducted on these animals demonstrated that approximately 6.2% ± 0.8% of prepro-HCRT-ir neurons were labeled for WGA ipsilaterally, and 3.4% ± 0.4% were labeled contralaterally (65% ipsilateral vs. 35% contralateral). Similarly to the case with infusions into the LC nucleus, HCRT neurons retrogradely labeled from the rostromedial pericoerulear dendritic zone were preferentially distributed within the dorsal half of the HCRT-ir cell group (67% ± 0.7% dorsal vs. 33% ± 1.2% ventral; n = 3).

In a limited number of cases, WGA infusions were observed outside of the LC region within Barrington's nucleus and the parabrachial nucleus. In two cases in which the infusion was located in Barrington's nucleus (Fig. 13; WGA 16 and 56), approximately 4.2% ± 1.1% of prepro-HCRT-ir neurons were labeled for WGA ipsilaterally and 2.8% ± 0.8% contralaterally (e.g., 60% ipsilateral labeling vs. 40% contralaterally). In one case in which the infusion was located in the medialmost aspect of the central lateral parabrachial subnucleus dorsolateral to LC (Fig. 13; WGA 41), approximately 5.0% ± 1.4% of prepro-HCRT-ir neurons were labeled for WGA ipsilaterally and 4.3% ± 1.4% contralaterally (54% ipsilateral labeling).

Dual retrograde labeling of HCRT neurons from individual basal forebrain regions and the LC

To examine the extent to which projections of individual HCRT neurons collateralize to the LC nucleus and to individual basal forebrain structures, 15 rats received infusions of both WGA into LC and FG into MS (n = 5), MPOA (n = 5), or SI (n = 5). WGA was identified by using silver intensification, and both FG and prepro-HCRT-ir neurons were identified by using immunoperoxidase techniques.

In cases in which FG was infused within MS, cell counts indicated that 29.6% ± 7.8% of prepro-HCRT-ir neurons retrogradely labeled from MS were also retrogradely labeled from LC (Fig. 4A,C,D). When collateralization was calculated relative to LC, 30.4% ± 3.0% of prepro-HCRT-ir neurons retrogradely labeled from LC were also retrogradely labeled from MS. In cases in which FG was infused within MPOA and WGA into LC, 34.1% ± 4.8% of the prepro-HCRT-ir neurons retrogradely labeled from MPOA were also retrogradely labeled from LC (Fig. 7A,C). Conversely, 27.8% ± 6.3% of prepro-HCRT-ir neurons retrogradely labeled from LC were also retrogradely labeled

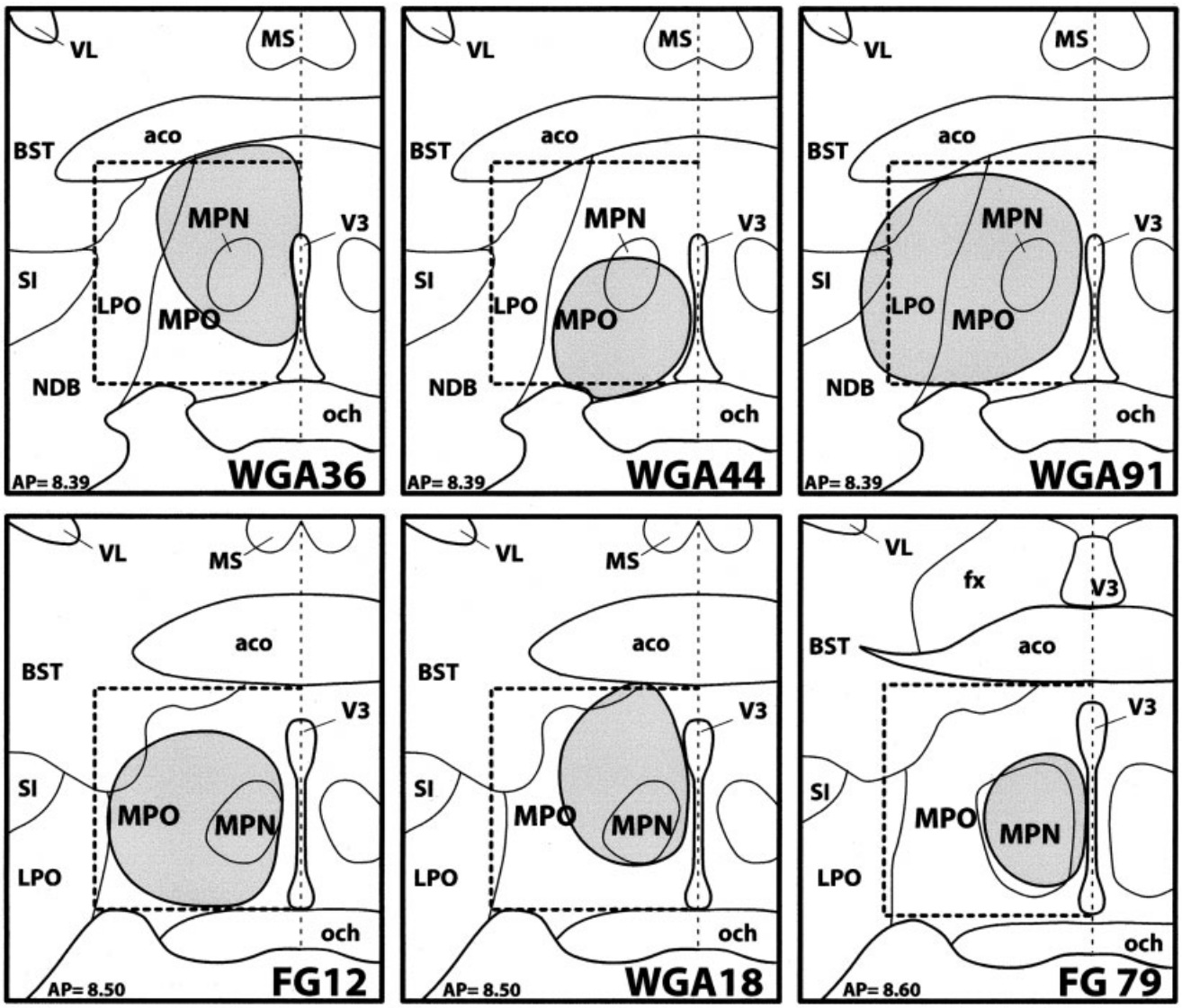

Fig. 6. Schematic depiction of approximate FG infusions within MPOA. Shown are locations of infusions within MPOA in six cases. The dashed lines denote the general area demonstrated previously as responsive to the wake-promoting actions of HCRT (España et al., 2001). aco, Anterior commissure; BST, bed nucleus of the stria terminalis; fx, fornix; LPO, lateral preoptic area; MPN, medial preoptic nucleus; MPO, medial preoptic area; MS, medial septum; och, optic chiasm; NDB, nucleus of the diagonal band; och, optic chiasm; SI, substantia innominata; V3, third ventricle; VL, lateral ventricle. Adapted from Swanson (1998).

from MPOA. In cases in which FG was infused within SI and WGA into LC, 29.2% ± 3.7% of prepro-HCRT-ir neurons retrogradely labeled from SI were also retrogradely labeled from LC (Fig. 10A,C). Conversely, 25.3% ± 2.2% of prepro-HCRT-ir neurons retrogradely labeled from LC were also retrogradely labeled from SI. For all combinations of FG and WGA infusions, relatively low levels of triple labeling were observed within the contralateral hemisphere.

Dual immunofluorescence retrograde labeling of HCRT neurons from two distinct basal forebrain regions

To examine whether projections of individual HCRT neurons collateralize to two distinct basal forebrain structures, 15 rats received infusions of both FG and CTb within two of the three basal forebrain regions described above (e.g., MS + MPOA, MS + SI, MPOA + SI). For any given pair of regions, tracer infusions were counterbalanced such that each region received each tracer. The following groups of animals were examined: 1a) FG in MS + CTb in MPOA (n = 2); 1b) CTb in MS + FG in MPOA (n = 2); 2a) FG in MS + CTb in SI (n = 2); 2b) CTb in MS + FG in SI (n = 3); 3a) FG in MPOA + CTb in SI (n = 3); and 3b) CTb in MPOA + FG in SI (n = 2). FG, CTb, and prepro-HCRT-ir neurons were identified by using immunofluorescence techniques. Infusions of FG or CTb within MS (n = 9), MPOA (n = 9), or SI (n = 10) were placed consistently within the general regions described above (see Figs. 2, 3, 5, 6, 8, 9 for examples).

Immunofluorescent analyses demonstrated that, in all regions examined, infusions of FG and CTb resulted in retrograde labeling throughout the HCRT-rich lateral hypothalamic region. In general, immunofluorescent staining of FG and CTb resulted in levels of retrograde labeling comparable to those observed with immunoperoxidase staining of FG. Nevertheless, in some cases examined, slightly higher levels of retrograde labeling were observed following CTb infusions compared with FG infusions (i.e., FG visualized either with immunoperoxidase or immunofluorescent labeling) within the ipsilateral and contralateral hemispheres. This difference in levels of retrograde labeling might be due, in part, to the infusion procedures used for each retrograde tracer (e.g., pressure vs. iontophoresis; see Discussion). Finally, the number of prepro-HCRT-ir neurons identified by using immunofluorescence was comparable to that observed with immunoperoxidase identification (data not shown).

To confirm that immunofluorescent techniques yielded retrograde labeling of prepro-HCRT-ir neurons comparable to that observed with immunoperoxidase-based procedures, double-label immunofluorescence was conducted on a subset of animals with moderate-sized to large (800–1,000 μm diameter) infusions of FG and CTb (e.g., HCRT + either FG or CTb). Levels of retrograde labeling of HCRT neurons obtained with immunofluorescent techniques following infusion of FG and CTb into MS, MPOA, and SI were comparable to those obtained using immunoperoxidase methods (compare Tables 1 and 2). Similarly to the case with immunoperoxidase methods, the majority of

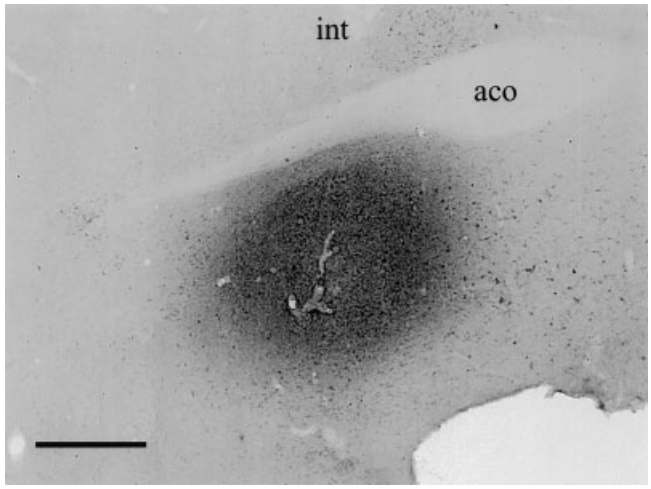

Fig. 8. Photomicrograph depicting a representative FG infusion within SI. Shown is a relatively large FG infusion within SI located immediately ventral to the anterior commissure and dorsal to the magnocellular preoptic area. Note the relatively well-demarcated border of the infusion with little diffusion into adjacent regions. aco, Anterior commissure; int, internal capsule. Scale bar = 400 μm.

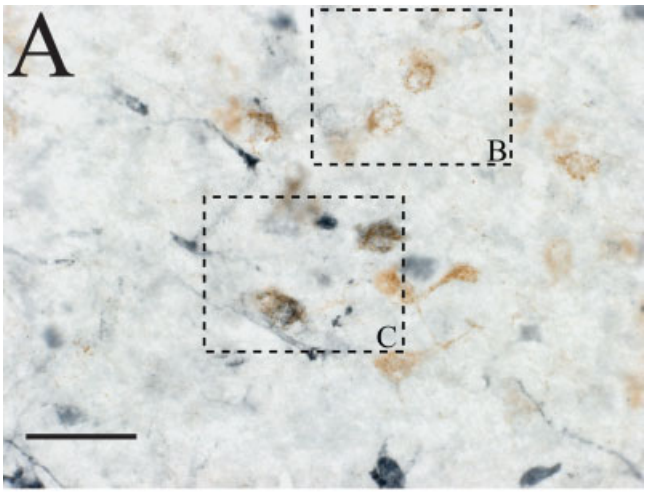

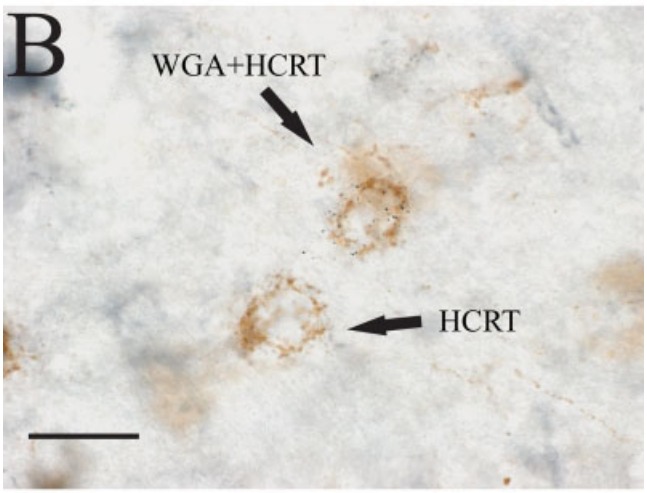

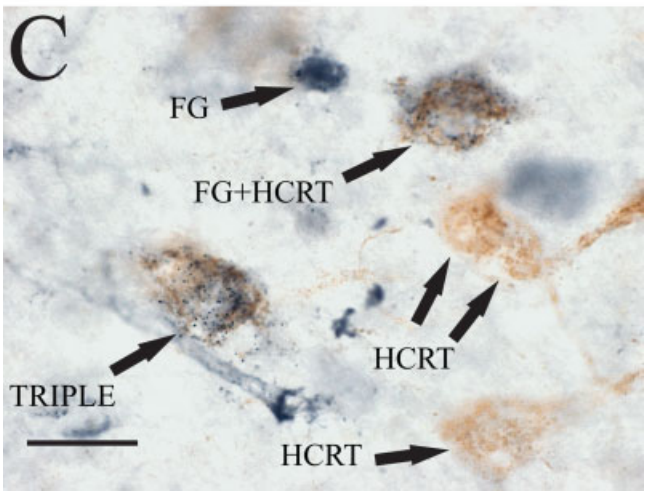

Fig. 7. Photomicrographs depicting retrogradely labeled and prepro-HCRT-ir neurons from one rat infused with FG in MPOA and with WGA in LC. Shown are FG labeled (FG; blue), prepro-HCRT-ir (HCRT; brown), and WGA labeled (WGA; black granules) within the perifornical region of the lateral hypothalamus. Boxes with corresponding letters in A indicate neurons displayed at higher magnification in B and C. **A:** Photomicrograph depicting individual HCRT neurons that project to MPOA (FG + HCRT), LC (WGA + HCRT), or both MPOA and LC (TRIPLE) as well as non-HCRT neurons that project to MPOA (FG). **B,C:** Photomicrographs of the same section as in A. Scale bars = 50 μm in A; 20 μm in B,C.

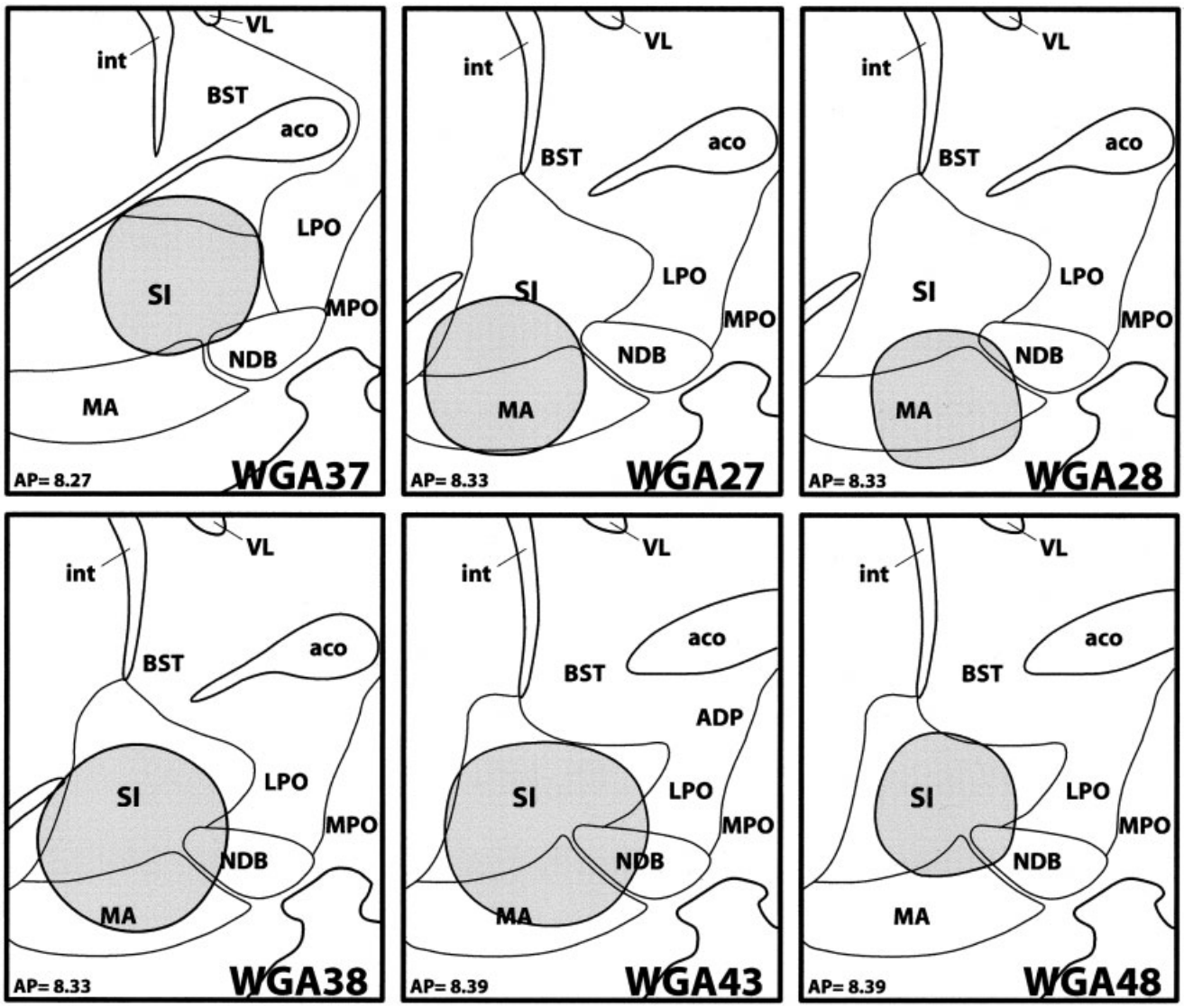

Fig. 9. Schematic depiction of the approximate location of FG infusions within SI. Shown are locations of FG infusion within SI in six rats. aco, Anterior commissure; BST, bed nucleus of the stria terminalis; int; internal capsule; LPO, lateral preoptic area; MA, magnocellular preoptic area; MPO, medial preoptic area; NDB, nucleus of the diagonal band; SI, substantia innominata; VL, lateral ventrical. Adapted from Swanson (1998).

retrograde labeling within HCRT-ir neurons was observed ipsilateral to the infusion site (Table 2).

Triple-label immunofluorescence was conducted in a subset of animals to examine collateralization of HCRT efferents to two distinct basal forebrain regions. These studies indicated that, in cases in which infusions were placed within both MS and MPOA, 29.0% ± 5.6% of prepro-HCRT-ir neurons retrogradely labeled from MS were also retrogradely labeled from MPOA. Conversely, 23.0% ± 3.3% of prepro-HCRT-ir neurons retrogradely labeled from MPOA were also retrogradely labeled from MS (Fig. 14, Table 3). In cases in which infusions were placed within MS and SI, 25.5% ± 3.3% of prepro-HCRT-ir neurons retrogradely labeled from MS were also retrogradely labeled from SI (Fig. 14, Table 3). Conversely, 29.0% ± 4.0% of prepro-HCRT-ir neurons retrogradely labeled from SI were also retrogradely labeled from MS. Finally, in cases in which infusions were placed within MPOA and SI, 19.2% ± 3.1% of prepro-HCRT-ir neurons retrogradely labeled from MPOA were also retrogradely labeled from SI. Conversely, 16.5% ± 3.0% of prepro-HCRT-ir neurons retrogradely labeled from SI were also retrogradely labeled from MPOA. For all combinations of FG and CTb infusions into these basal forebrain structures, relatively low levels of labeling were observed within the contralateral hemisphere (Table 3).

DISCUSSION

Evidence suggests that the hypocretins modulate behavioral state via actions across multiple terminal fields. Thus, HCRT-containing fibers and HCRT receptors are

located within a variety of arousal-related regions (Peyron et al., 1998). Infusion of HCRT directly within a number of basal forebrain and brainstem regions elicits increases in time spent awake and behavioral activation (Bourgin et al., 2000; Methippara et al., 2000; Thakkar et al., 2001; España et al., 2001). Prior to the current study, little was known regarding the anatomical organization of HCRT efferents to these structures. This lack of information regarding the basic organizational features of HCRT efferents across multiple HCRT terminal fields represented a substantial deficiency in our understanding of the neurobiology of this neurotransmitter system.

To characterize better the anatomical organization of HCRT efferents to basal forebrain and brainstem arousal-related regions, the current studies utilized single- and double-retrograde labeling of immunohistochemically identified HCRT neurons. In these studies, unilateral infusions of retrograde tracers were made into basal forebrain and brainstem regions previously demonstrated to be sensitive to the behavioral-state-modulatory actions of HCRT. It was observed that infusions of FG or CTb within the basal forebrain regions, MS, MPOA and SI, resulted in moderate labeling of HCRT-ir neurons ipsilaterally and substantially less labeling contralaterally. Additionally, these studies suggest the possibility of a slight preferential distribution of basal-forebrain-projecting HCRT neurons within the medial portion of the HCRT cell group.

In contrast to the case with infusions into the basal forebrain, infusions into LC (nucleus and pericoerulear dendritic zones) resulted in considerably more labeling bilaterally within HCRT neurons, albeit with an ipsilateral bias (e.g., approximately 2:1 ipsilateral:contralateral). Additionally, there appeared to be a stronger topographic organization of HCRT neurons that projected to either LC proper or the rostromedial pericoerulear dendritic zone, with nearly two-thirds of these neurons located within the dorsal half of the HCRT-ir group. Additionally, somewhat greater labeling was also observed within the medial half of the HCRT-ir cell group. Comparison of results obtained with WGA infusions into and outside the region of LC, including within Barrington's nucleus and the central lateral parabrachial nucleus, suggest the hypothesis that brainstem structures in general may receive a greater proportion of HCRT input from the contralateral hemisphere than do basal forebrain structures.

The current studies also examined the degree to which individual HCRT neurons collateralize to target more than one of these terminal fields. It was observed that a substantial proportion of individual HCRT neurons that project to one of the behavioral state-related terminal fields examined in this study simultaneously projects to other arousal-related regions. Consistent with the largely ipsilateral nature of HCRT projections to the basal forebrain, HCRT neurons labeled simultaneously from both the basal forebrain and the LC were observed primarily within the ipsilateral HCRT cell group. A similar magni-

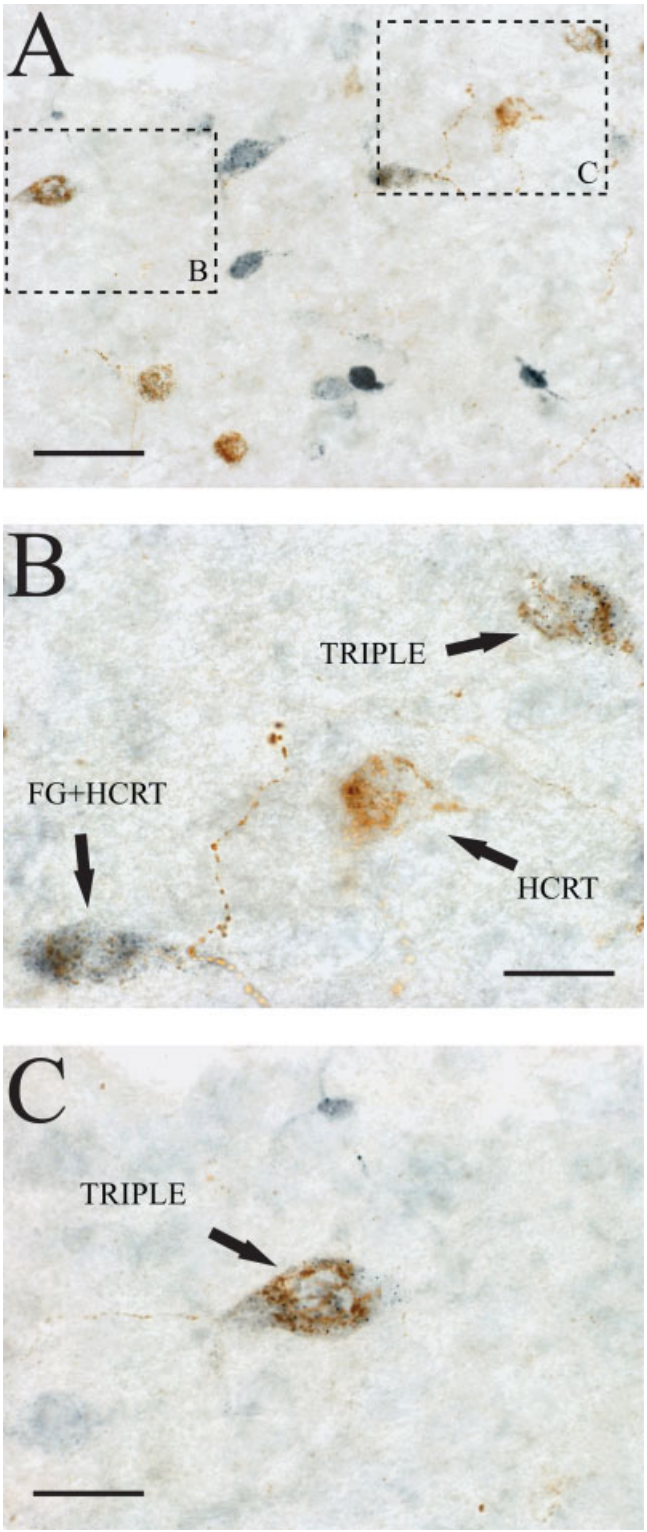

Fig. 10. Photomicrographs depicting retrogradely labeled and HCRT-ir neurons from one rat infused with FG in SI and with WGA in LC. Shown are FG labeled (FG; blue), HCRT-ir (HCRT; brown), and WGA labeled (WGA; black granules) neurons within the perifornical region of the lateral hypothalamus. Boxes with corresponding letters in A indicate neurons displayed at higher magnification in B and C. **A:** Photomicrograph depicting individual HCRT neurons that project to SI (FG + HCRT), LC (WGA + HCRT), or both SI and LC (triple) as well as non-HCRT neurons that project to SI (FG). **B,C:** Photomicrographs of the same section as in A. Scale bars = 50 μm in A; 20 μm in B,C.

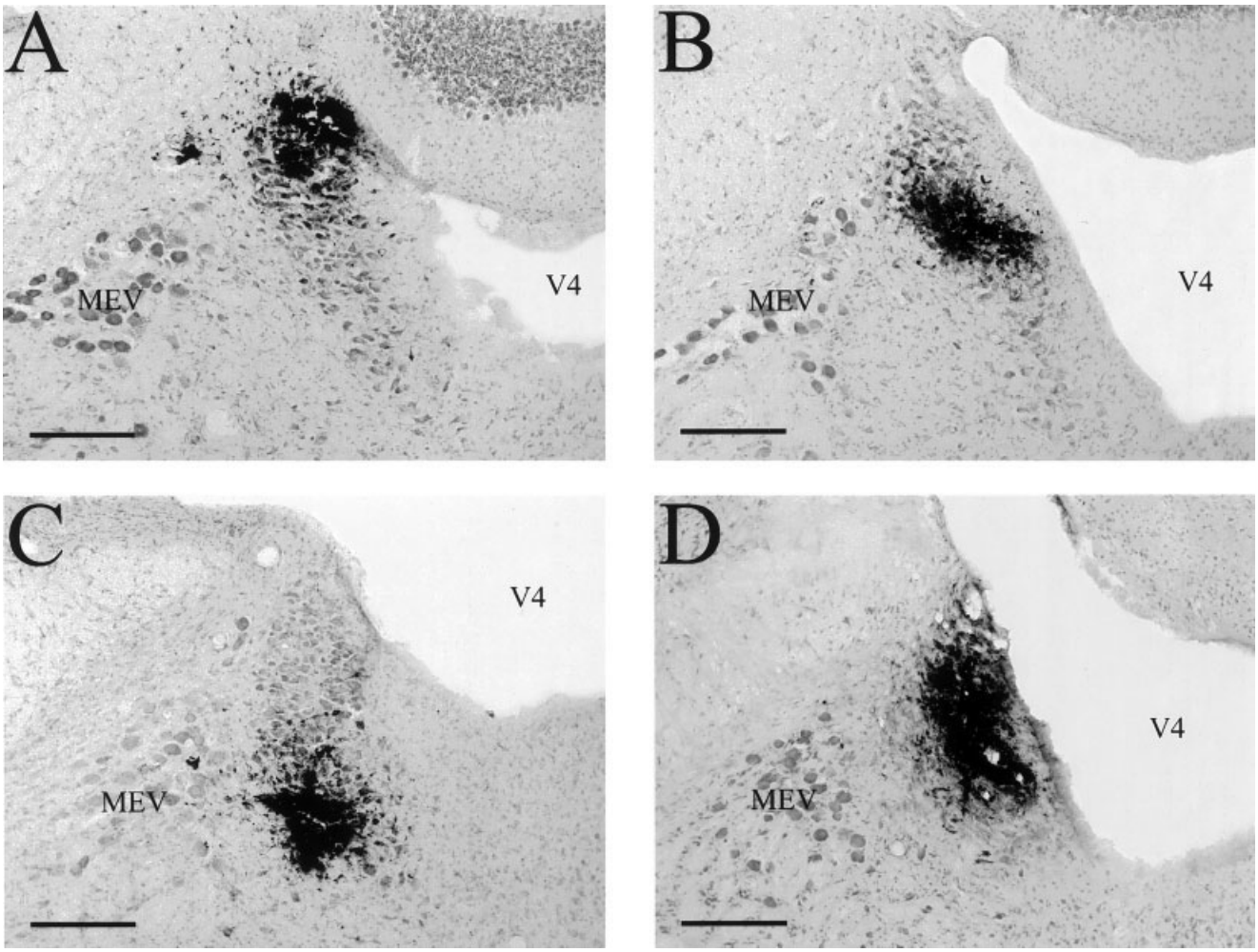

Fig. 11. Photomicrographs depicting representative WGA infusions within LC. Shown are WGA infusions that filled approximately 30–90% of LC in four separate animals (**A–D**). Note the relatively well-demarcated borders of the WGA infusions with little diffusion into adjacent regions. MEV, mesencephalic nucleus of the trigeminal; V4, fourth ventricle. Scale bars = 200 μm.

tude of collateralization of HCRT efferents to two distinct basal forebrain regions (e.g., MS and MPOA) was also observed.

Methodological considerations

Infusion volume is a critical variable in the use of retrograde tracers (Ader et al., 1980). In the current study, infusion volumes were used that resulted in diffusion of tracer throughout a substantial portion of the targeted region, while avoiding diffusion of tracer into adjacent structures. The use of infusions of WGA, FG, or CTb that did not entirely fill the targeted structure likely results in an underestimation of the absolute number of HCRT neurons projecting to a given structure. None of the retrograde tracer infusions filled more than one-half of any given region, and most filled substantially less than this. Thus, it is estimated that at least two to three times higher levels of retrograde labeling of HCRT neurons would have been observed had an entire terminal field been filled with retrograde tracer. Prevention of diffusion of tracer outside LC was of primary concern, given the small size of the LC nucleus and the close proximity of this nucleus to a variety of brainstem structures implicated in the regulation of state and state-dependent processes. For this reason, relatively small infusions of WGA were used that resulted in highly restricted distribution of the tracer in the rostrocaudal, mediolateral, and dorsoventral dimensions. Nevertheless, in a limited number of cases, WGA infusions were observed outside of the LC region. In general, these infusions resulted in diminished levels of labeling within HCRT neurons relative to those obtained with infusions into the LC nucleus and the LC dendritic zone.

In the case of MS, MPOA, and SI, previous mapping studies indicate wake-promoting actions of HCRT and other neurotransmitters within these general regions of the basal forebrain (Kumar et al., 1986; Mallick and Alam, 1992; Berridge and Foote, 1996; Berridge et al., 1996, 1999, 2003; Berridge and O'Neill, 2001; Thakkar et al., 2001; España et al., 2001). As defined in previous studies, these regions are relatively large and anatomically complex. Thus, the region defined as MS and identified as

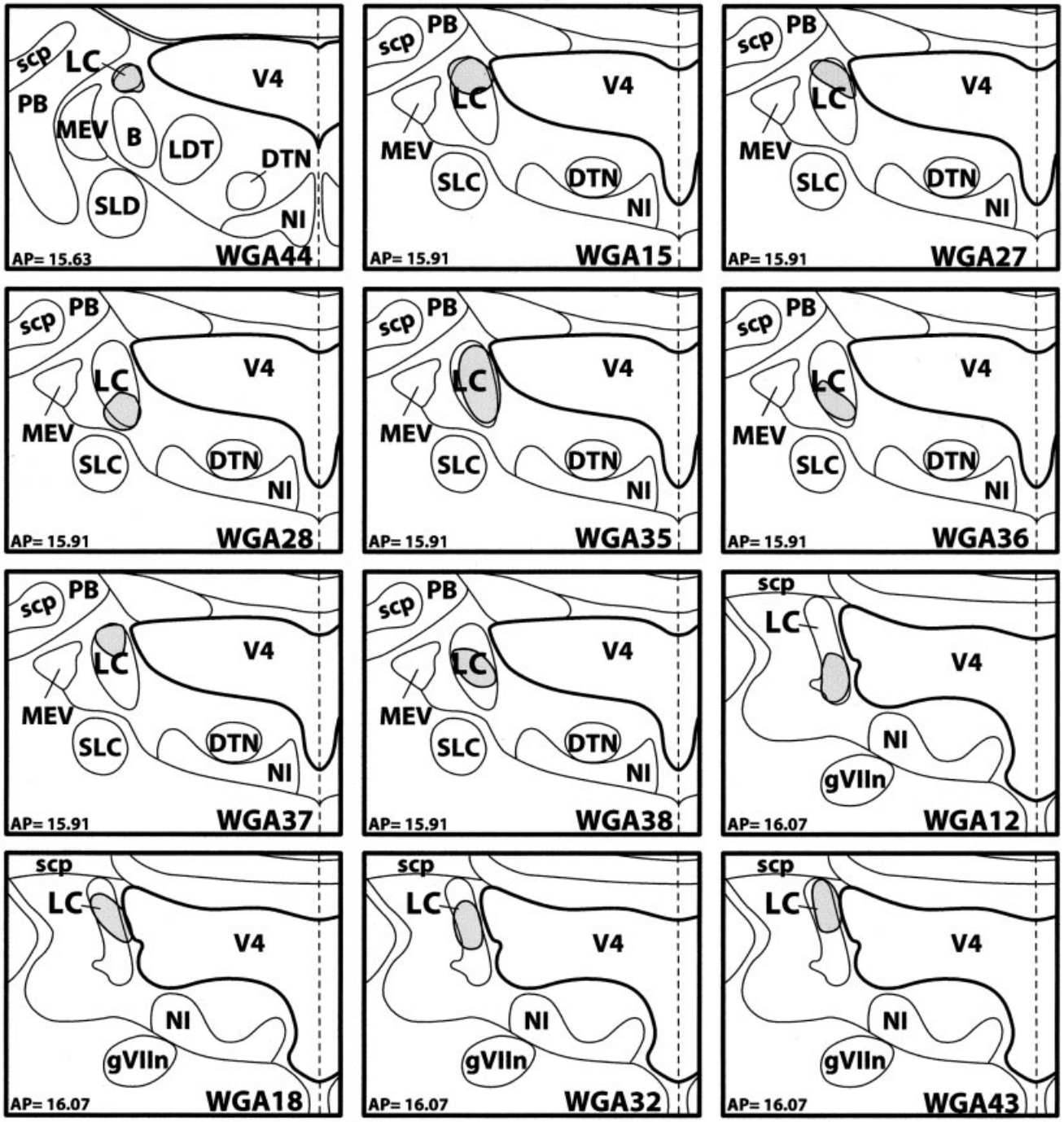

Fig. 12. Schematic depictions of approximate WGA infusion locations within LC. Shown are representative infusion locations within LC in 12 separate rats. B, Barrington's nucleus; DTN; dorsal tegmental nucleus; gVIIn, genu of the facial nerve; LC, locus coeruleus; LDT; laterodrosal tegmental nucleus; MEV, mesencephalic nucleus of the trigeminal; NI, nucleus incertus; PB, parabrachial nucleus; scp, superior cerebellar peduncle; SLC, subcoeruleus nucleus; SLD, sublaterodorsal nucleus; V4, fourth ventrical. Adapted from Swanson (1998).

being sensitive to the wake-promoting actions of HCRT encompasses the medial septum, the vertical limb of the diagonal band of Broca, the islands of Calleja, and relatively small portions of LPO (Swanson, 1998). In the case of wake-promoting actions of HCRT within MPOA, this region encompasses the MPO; the medial, median, anterodorsal, and anteroventral preoptic nuclei; and the anteroventral periventricular nucleus of the hypothalamus (Swanson, 1998). The current experiments were aimed at a better of understanding the anatomical organization

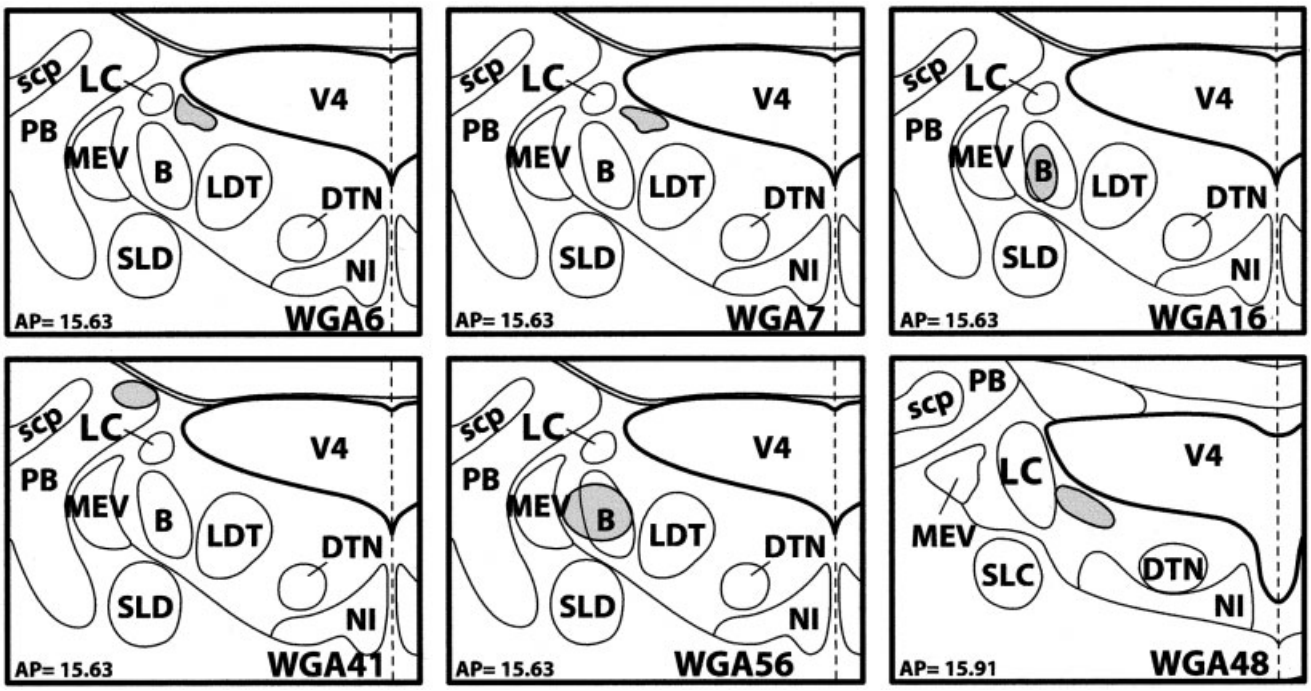

Fig. 13. Schematic depictions of approximate WGA infusion locations within several pericoerulear regions. Shown are representative infusion locations within the rostromedial pericoerulear zone, Barrington's nucleus, and the parabrachial nucleus. B, Barrington's nucleus; DTN; dorsal tegmental nucleus; LC, locus coeruleus; LDT; laterodrosal tegmental nucleus; MEV, mesencephalic nucleus of the trigeminal; NI, nucleus incertus; PB, parabrachial nucleus; scp, superior cerebellar peduncle; SLC, subcoeruleus nucleus; SLD, sublaterodorsal nucleus; V4, fourth ventrical. Adapted from Swanson (1998).

TABLE 2. Mean Number and Percentage of HCRT Neurons Retrogradely Labeled with FG or CTb from Individual Basal Forebrain Regions[1]

	Ipsilateral		Contralateral	
	Mean	Percentage	Mean	Percentage
MS (FG + HCRT)	5.8 ± 1.2	7.1 ± 1.4	1.1 ± 0.5	1.2 ± 0.6
MS (CTb + HCRT)	11.8 ± 1.6	10.4 ± 0.9	5.7 ± 1.2	5.2 ± 1.0
MPOA (FG + HCRT)	7.3 ± 1.6	9.1 ± 1.5	2.8 ± 0.5	2.7 ± 0.4
MPOA (CTb + HCRT)	7.0 ± 0.9	8.2 ± 1.5	2.3 ± 0.4	2.8 ± 0.6
SI (FG + HCRT)	6.6 ± 0.9	6.1 ± 0.8	1.0 ± 0.3	0.9 ± 0.3
SI (CTb + HCRT)	8.5 ± 1.3	10.7 ± 1.3	2.3 ± 0.5	2.1 ± 0.3

[1]Mean (±SEM) number and percentage (±SEM) of HCRT-ir neurons that were retrogradely labeled from individual basal forebrain regions (MS, MPOA, or SI) with FG (FG + HCRT) or CTb (CTb + HCRT).

underlying the wake-promoting actions of HCRT within these general basal forebrain regions. As such, these studies utilized moderately large infusions that resulted in distribution of retrograde tracer throughout a substantial portion of a given region previously identified as being sensitive to the wake-promoting actions of HCRT. It remains for future studies, using more restricted tracer infusions, to characterize HCRT efferents to individual subnuclei contained within these general regions.

For FG infusions into MS, in some cases infusate might have encroached on the medial portion of nucleus accumbens. However, in one case in which an FG infusion was made directly into the nucleus accumbens (shell and core) while avoiding more medial structures, including the medial septum and NDB, low levels of retrograde labeling were observed within HCRT neurons. Thus, it does not appear that uptake of retrograde tracer from either shell or core subregions of the nucleus accumbens contributes substantially to the labeling of HCRT neurons observed following infusions into MS. In the case of MPOA, all infusions were concentrated within the medial portions of this general region, with little diffusion into the bed nucleus of the stria terminalis or LPO. Comparable patterns and density of labeling were observed following infusions into medial, lateral, dorsal, and ventral portions of MPOA. Infusions that targeted SI were well contained within the borders of this region and did not result in diffusion outside of the SI region. Nevertheless, in two cases, infusions of FG were made within ventral portions of SI and resulted in substantial diffusion of FG into the posterior horizontal limb of the diagonal band of Broca and the magnocellular preoptic nucleus. In these two cases, however, retrograde labeling within LH appeared to be indistinguishable from that observed with infusions placed more dorsally within SI. Despite the use of moderately large infusions of FG and CTb, in no case did these infusions completely fill any of the basal forebrain regions previously defined as being sensitive to the wake-promoting actions of HCRT. Thus, as mentioned above, the current study most likely underestimates the absolute number of HCRT neurons projecting to these regions.

An additional potential confound with retrograde tracers is the possible uptake and transport by fibers of passage. Previous studies suggest that axonal uptake is unlikely with WGA, insofar as injection of this tracer into peripheral or central fiber tracts results in little or no retrograde labeling (Menetrey, 1985; Basbaum and Menetrey, 1987). In contrast to WGA, it is generally accepted

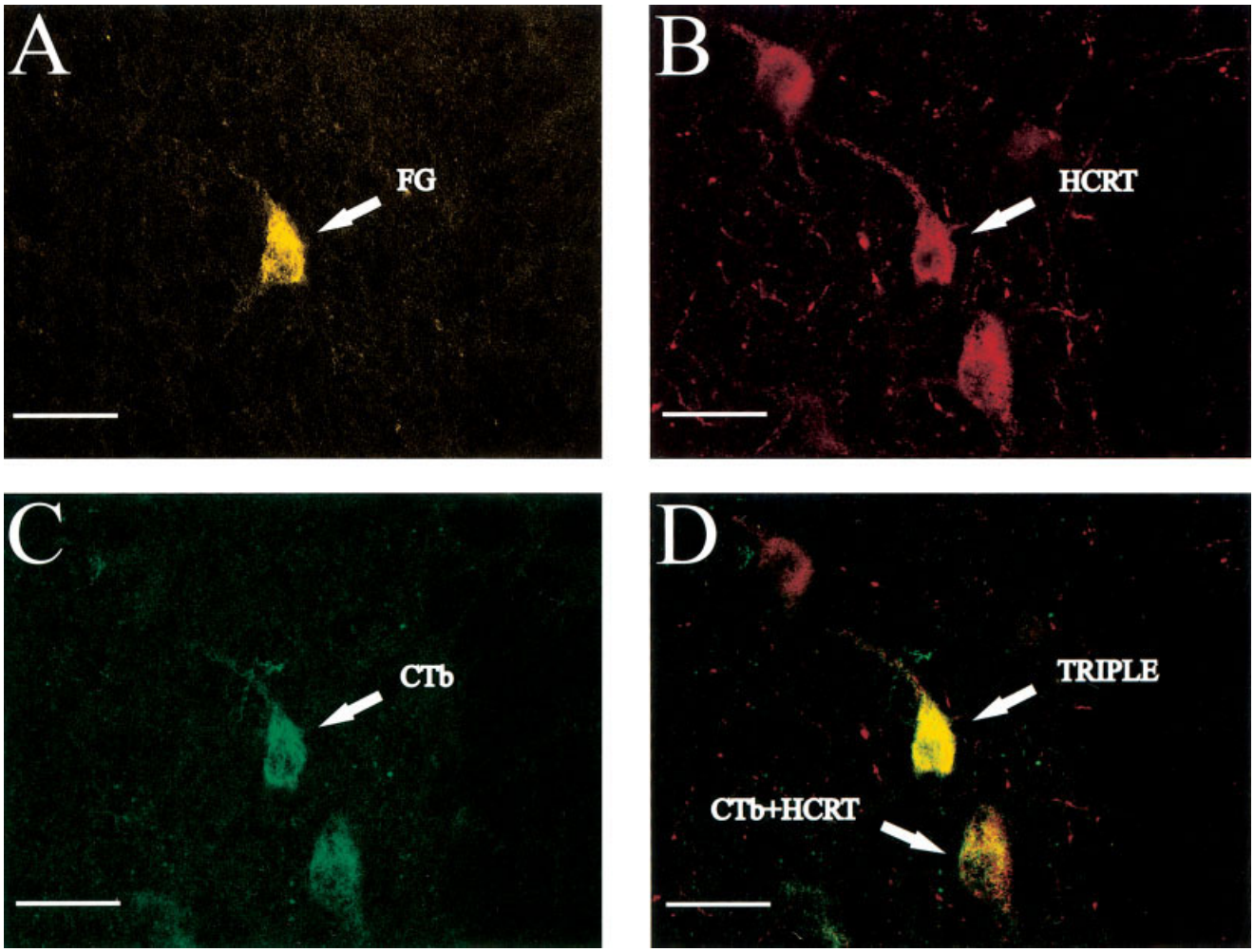

Fig. 14. Fluorescent photomicrographs depicting retrogradely labeled and HCRT-ir neurons from one rat infused with FG in MS and with CTb in MPOA. Shown are photomicrographs depicting FG-labeled (**A**; yellow/gold), HCRT-ir (**B**; red), and CTb-labeled (**C**; green) neurons within the perifornical region of the lateral hypothalamus. **D** is a composite of A–C, showing an HCRT-ir neuron that is retrogradely labeled from MPOA (CTb + HCRT) and an additional HCRT-ir neuron retrogradely labeled from both MS and MPOA (triple). Arrows point to this triple-labeled neuron. Scale bars = 125 μm.

TABLE 3. Percentage of Basal-Forebrain-Projecting HCRT Neurons Retrogradely Labeled from a Second Basal Forebrain Region[1]

	Ipsilateral	Contralateral
MS + MPOA	29.0 ± 5.6	3.8 ± 2.9
MPOA + MS	23.3 ± 3.3	7.9 ± 3.8
MS + SI	25.5 ± 3.3	5.2 ± 2.8
SI + MS	29.0 ± 4.0	8.8 ± 4.0
MPOA + SI	19.2 ± 3.1	5.2 ± 3.0
SI + MPOA	16.5 ± 3.0	9.7 ± 6.1

[1]Shown are the percentage (±SEM) of HCRT neurons that project to one basal forebrain region (MS, MPOA, or SI) that are also retrogradely labeled from a second basal forebrain region (+MS, +MPOA, +SI; see Results). Percentage collateralization is expressed relative to each structure for any give pair of structures. For example, in the case of infusion of tracers into MS and MPOA, the percentage of MS-projecting neurons also projecting to MPOA (MS + MPOA) and the percentage of MPOA-projecting neurons also projecting to MS (MPOA + MS) are presented.

that FG and CTb, as well as many other retrograde tracers, can be taken up by fibers of passage, although this appears to be minimal with iontophoretic application compared with pressure injection (Pieribone and Aston-Jones, 1988). Thus, the slightly higher levels of retrograde labeling observed in the current studies with CTb pressure ejection vs. FG iontophoretic ejection might in part reflect variations in the degree to which these tracers were taken up by fibers of passage. However, the fact that both qualitatively and quantitatively similar patterns of retrograde labeling were observed with iontophoretic and pressure ejection of tracers suggests that results obtained in the present study accurately reflect the pattern of HCRT efferents to these basal forebrain regions.

Functional implications

HCRT-containing fibers and HCRT receptors are located within a variety of basal forebrain and brainstem regions, including, LC, MS, MPOA, and SI (Peyron et al., 1998; Sakurai et al., 1998; Date et al., 1999; Nambu et al., 1999; Taheri et al., 1999; Bourgin et al., 2000; Greco and Shiromani, 2001; Marcus et al., 2001; Hervieu et al., 2001; Backberg et al., 2002; Cluderay et al., 2002; Suzuki et al., 2002). Each of these regions has been implicated in the

regulation of behavioral state and state-dependent processes (Hobson et al., 1975; Foote et al., 1980; Kumar et al., 1986; Buzsaki et al., 1988; Metherate et al., 1992; Mallick and Alam, 1992; Berridge and Foote, 1996; Berridge and O'Neill, 2001). Infusion of HCRT-1 directly into each of these regions elicits robust increases in waking and reductions in slow-wave and rapid-eye-movement (REM) sleep (Bourgin et al., 2000; Thakkar et al., 2001; España et al., 2001). These changes in sleep-wake state are accompanied by alterations in a variety of state-dependent behavioral activities (España et al., 2001).

A question raised by these observations is the degree to which the activity of HCRT efferents across terminal fields is independently regulated. One possibility is that the actions of HCRT on arousal state and/or state-dependent processes involve the simultaneous activation of HCRT efferents to diverse brainstem and basal forebrain structures involved in the regulation of state and state-dependent processes. Alternatively, HCRT neurons that project to specific terminal fields might be differentially activated/regulated, depending on physiological and environmental conditions. A distinct topographic organization of HCRT neurons with respect to terminal field projections might suggest segregated input to subpopulations of HCRT neurons and the differential regulation of HCRT efferents across multiple terminal fields. In the current studies, basal-forebrain-projecting HCRT neurons did not display a strong topographic organization. This could suggest that HCRT neurons that project to distinct basal forebrain terminal fields are not differentially regulated. This conclusion is consistent with the observation that a large percentage of basal-forebrain-projecting HCRT neurons target more than one basal forebrain terminal field. In contrast to the basal forebrain, a stronger topographic organization of LC-projecting HCRT neurons was observed, with approximately two-thirds of these neurons located within the dorsal half of the HCRT cell group. Thus, it is possible that, under certain conditions, LC-projecting HCRT neurons may be differentially regulated relative to basal-forebrain-projecting HCRT neurons. Nonetheless, among individual LC-projecting HCRT neurons, a large percentage simultaneously projects to a basal forebrain structure. It will be of interest for future studies to determine the degree to which afferent input to the HCRT group displays a similar topographic organization.

Combined, these observations suggest that the organization of the HCRT efferent system results in the coordinated (e.g., simultaneous) actions of HCRT across multiple anatomically distinct, yet functionally related, basal forebrain and brainstem terminal fields. Of course, the terminal fields examined in the current study support a diversity of distinct, nonoverlapping functions. Thus, the collateralization of HCRT efferents to these regions reflects coordinated actions of HCRT across functionally distinct terminal fields. Nonetheless, these four terminal fields share the ability to modulate sleep-wake state when individually manipulated by a variety of pharmacological treatments. To date, all studies examining the potential role of HCRT within these basal forebrain and brainstem regions have examined the sleep-wake effects of HCRT infusion into one terminal field only. A critical question for future studies is what are the quantitative and qualitative behavioral modulatory actions of HCRT when simultaneously applied to two or more of these terminal fields.

HCRT efferents to basal forebrain regions are largely ipsilateral. This could suggest hemisphere-dependent actions of HCRT that could be differentially regulated. In contrast to what is observed with basal forebrain efferents, HCRT projections to LC and other dorsal pontine structures are more bilateral in nature. It is interesting that this pattern of predominantly ipsilateral projections to forebrain and bilateral projections to brainstem is similar to that observed with LC, another ascending modulatory transmitter system implicated in the regulation of behavioral state (Waterhouse et al., 1983; Simpson et al., 1997).

The current studies limited examination of HCRT efferent projections to a subset of HCRT terminal fields previously demonstrated to participate in HCRT-induced alterations in behavioral state (España et al., 2001). It remains for future studies to characterize HCRT efferent projections to other arousal-related and nonarousal-related HCRT terminal fields. In addition to MPOA, a variety of hypothalamic structures have been implicated in the regulation of behavioral state (Sallanon et al., 1987; Sherin et al., 1996; Lu et al., 2000, 2002). It will be of particular interest to characterize better the behavioral state modulatory actions of HCRT within these structures and to characterize the HCRT efferent system to these regions. Finally, HCRT projects widely throughout the brain, targeting a variety of structures implicated in a variety of behavioral processes. Thus, it will be important to compare the organization of HCRT efferents to arousal-related and arousal-independent structures.

In summary, the present studies demonstrate that HCRT efferents to individual basal forebrain regions arise primarily from neurons located within the ipsilateral HCRT cell group. In contrast, HCRT neurons that project to LC appear to project in a bilateral manner, albeit with an ipsilateral bias. Additionally, LC-projecting HCRT neurons appear to be distributed preferentially within the dorsal HCRT group. Finally, individual HCRT neurons simultaneously target multiple basal forebrain/brainstem structures involved in HCRT-induced increases in waking and behavioral activity. Together these observations suggest a broadly projecting efferent system, which ensures coordinated actions across functionally related terminal fields.

LITERATURE CITED

Ader JP, Room P, Postema F, Korf J. 1980. Bilaterally diverging axon collaterals and contralateral projections from rat locus coeruleus neurons, demonstrated by fluorescent retrograde double labeling and norepinephrine metabolism. J Neural Transm 49:207–208.

Arnsten AF, Goldman-Rakic PS. 1984. Selective prefrontal cortical projections to the region of the locus coeruleus and raphe nuclei in the rhesus monkey. Brain Res 306:9–18.

Backberg M, Hervieu G, Wilson S, Meister B. 2002. Orexin receptor-1 (OX-R1) immunoreactivity in chemically identified neurons of the hypothalamus: focus on orexin targets involved in control of food and water intake. Eur J Neurosci 15:315–328.

Basbaum AI, Menetrey D. 1987. Wheat germ agglutinin-apoHRP gold: a new retrograde tracer for light- and electron-microscopic single- and double-label studies. J Comp Neurol 261:306–318.

Berridge CW, Foote SL. 1996. Enhancement of behavioral and electroencephalographic indices of waking following stimulation of noradrenergic beta-receptors within the medial septal region of the basal forebrain. J Neurosci 16:6999–7009.

Berridge CW, O'Neill J. 2001. Differential sensitivity to the wake-promoting actions of norepinephrine within the medial preoptic area and the substantia innominata. Behav Neurosci 115:165–174.

Berridge CW, Bolen SJ, Manley MS, Foote SL. 1996. Modulation of forebrain electroencephalographic activity in halothane-anesthetized rat via actions of noradrenergic beta-receptors within the medial septal region. J Neurosci 16:7010–7020.

Berridge CW, O'Neil J, Wifler K. 1999. Amphetamine acts within the medial basal forebrain to initiate and maintain alert waking. Neuroscience 93:885–896.

Berridge CW, Isaac SO, España RA. 2003. Additive wake-promoting actions of medial basal forebrain noradrenergic alpha1- and beta-receptor stimulation. Behav Neurosci 117:350–359.

Bourgin P, Huitron-Resendiz S, Spier AD, Fabre V, Morte B, Criado JR, Sutcliffe JG, Henriksen SJ, de Lecea L. 2000. Hypocretin-1 modulates rapid eye movement sleep through activation of locus coeruleus neurons. J Neurosci 20:7760–7765.

Buzsaki G, Bickford RG, Ponomareff G, Thal LJ, Mandel R, Gage FH. 1988. Nucleus basalis and thalamic control of neocortical activity in the freely moving rat. J Neurosci 8:4007–4026.

Chemelli RM, Willie JT, Sinton CM, Elmquist JK, Scammell T, Lee C, Richardson JA, Williams SC, Xiong Y, Kisanuki Y, Fitch TE, Nakazato M, Hammer RE, Saper CB, Yanagisawa M. 1999. Narcolepsy in orexin knockout mice: molecular genetics of sleep regulation. Cell 98:437–451.

Cluderay JE, Harrison DC, Hervieu GJ. 2002. Protein distribution of the orexin-2 receptor in the rat central nervous system. Regul Pept 104: 131–144.

Date Y, Ueta Y, Yamashita H, Yamaguchi H, Matsukura S, Kangawa K, Sakurai T, Yanagisawa M, Nakazato M. 1999. Orexins, orexigenic hypothalamic peptides, interact with autonomic, neuroendocrine and neuroregulatory systems. Proc Natl Acad Sci U S A 96:748–753.

Drolet G, Van Bockstaele EJ, Aston-Jones G. 1992. Robust enkephalin innervation of the locus coeruleus from the rostral medulla. J Neurosci 12:3162–3174.

España RA, Baldo BA, Kelley AE, Berridge CW. 2001. Wake-promoting and sleep-suppressing actions of hypocretin (orexin): basal forebrain sites of action. Neuroscience 106:699–715.

España RA, Plahn S, Berridge CW. 2002. Circadian-dependent and circadian-independent behavioral actions of hypocretin/orexin. Brain Res 943:224–236.

España RA, Valentino RJ, Berridge CW. 2003. Fos immunoreactivity in hypocretin-synthesizing and hypocretin-1 receptor-expressing neurons: effects of diurnal and nocturnal spontaneous waking, stress and hypocretin-1 administration. Neuroscience 121:201–217.

Foote SL, Aston-Jones G, Bloom FE. 1980. Impulse activity of locus coeruleus neurons in awake rats and monkeys is a function of sensory stimulation and arousal. Proc Natl Acad Sci U S A 77:3033–3037.

Greco MA, Shiromani PJ. 2001. Hypocretin receptor protein and mRNA expression in the dorsolateral pons of rats. Brain Res Mol Brain Res 88:176–182.

Hagan JJ, Leslie RA, Patel S, Evans ML, Wattam TA, Holmes S, Benham CD, Taylor SG, Routledge C, Hemmati P, Munton RP, Ashmeade TE, Shah AS, Hatcher JP, Hatcher PD, Jones DN, Smith MI, Piper DC, Hunter AJ, Porter RA, Upton N. 1999. Orexin A activates locus coeruleus cell firing and increases arousal in the rat. Proc Natl Acad Sci U S A 96:10911–10916.

Hervieu GJ, Cluderay JE, Harrison DC, Roberts JC, Leslie RA. 2001. Gene expression and protein distribution of the orexin-1 receptor in the rat brain and spinal cord. Neuroscience 103:777–797.

Hobson JA, McCarley RW, Wyzinski PW. 1975. Sleep cycle oscillation: reciprocal discharge by two brainstem neuronal groups. Science 189: 55–58.

Ida T, Nakahara K, Katayama T, Murakami N, Nakazato M. 1999. Effect of lateral cerebroventricular injection of the appetite-stimulating neuropeptide, orexin and neuropeptide Y, on the various behavioral activities of rats. Brain Res 821:526–529.

Kumar VM, Datta S, Chhina GS, Singh B. 1986. Alpha adrenergic system in medial preoptic area involved in sleep-wakefulness in rats. Brain Res Bull 16:463–468.

Lin L, Faraco J, Li R, Kadotani H, Rogers W, Lin X, Qiu X, de Jong PJ, Nishino S, Mignot E. 1999. The sleep disorder canine narcolepsy is caused by a mutation in the hypocretin (orexin) receptor 2 gene. Cell 98:365–376.

Lu J, Greco MA, Shiromani P, Saper CB. 2000. Effect of lesions of the ventrolateral preoptic nucleus on NREM and REM sleep. J Neurosci 20:3830–3842.

Lu J, Bjorkum AA, Xu M, Gaus SE, Shiromani PJ, Saper CB. 2002. Selective activation of the extended ventrolateral preoptic nucleus during rapid eye movement sleep. J Neurosci 22:4568–4576.

Mallick BN, Alam MN. 1992. Different types of norepinephrinergic receptors are involved in preoptic area mediated independent modulation of sleep-wakefulness and body temperature. Brain Res 591:8–19.

Marcus JN, Aschkenasi CJ, Lee CE, Chemelli RM, Saper CB, Yanagisawa M, Elmquist JK. 2001. Differential expression of orexin receptors 1 and 2 in the rat brain. J Comp Neurol 435:6–25.

Menetrey D. 1985. Retrograde tracing of neural pathways with a protein-gold complex. I. Light microscopic detection after silver intensification. Histochemistry 83:391–395.

Mesulam MM, Mufson EJ, Wainer BH, Levey AI. 1983. Central cholinergic pathways in the rat: an overview based on an alternative nomenclature (Ch1–Ch6). Neuroscience 10:1185–1201.

Metherate R, Cox CL, Ashe JH. 1992. Cellular bases of neocortical activation: modulation of neural oscillations by the nucleus basalis and endogenous acetylcholine. J Neurosci 12:4701–4711.

Methippara MM, Alam MN, Szymusiak R, McGinty D. 2000. Effects of lateral preoptic area application of orexin-A on sleep-wakefulness. Neuroreport 11:3423–3426.

Nambu T, Sakurai T, Mizukami K, Hosoya Y, Yanagisawa M, Goto K. 1999. Distribution of orexin neurons in the adult rat brain. Brain Res 827:243–260.

Nishino S, Ripley B, Overeem S, Lammers GJ, Mignot E. 2000. Hypocretin (orexin) deficiency in human narcolepsy. Lancet 355:39–40.

Peyron C, Tighe DK, van Den Pol AN, de Lecea L, Heller HC, Sutcliffe JG, Kilduff TS. 1998. Neurons containing hypocretin (orexin) project to multiple neuronal systems. J Neurosci 18:9996–10015.

Pickel VM, Joh TH, Reis DJ. 1977. A serotonergic innervation of noradrenergic neurons in nucleus locus coeruleus: demonstration by immunocytochemical localization of the transmitter specific enzymes tyrosine and tryptophan hydroxylase. Brain Res 131:197–214.

Pieribone VA, Aston-Jones G. 1988. The iontophoretic application of fluorogold for the study of afferents to deep brain nuclei. Brain Res 475:259–271.

Piper DC, Upton N, Smith MI, Hunter AJ. 2000. The novel brain neuropeptide, orexin-A, modulates the sleep-wake cycle of rats. Eur J Neurosci 12:726–730.

Sakurai T, Amemiya A, Ishii M, Matsuzaki I, Chemelli RM, Tanaka H, Williams SC, Richarson JA, Kozlowski GP, Wilson S, Arch JR, Buckingham RE, Haynes AC, Carr SA, Annan RS, McNulty DE, Liu WS, Terrett JA, Elshourbagy NA, Bergsma DJ, Yanagisawa M. 1998. Orexins and orexin receptors: a family of hypothalamic neuropeptides and G protein-coupled receptors that regulate feeding behavior. Cell 92:1.

Sallanon M, Kitahama K, Buda C, Puymartin M, Luppi PH, Jouvet M. 1987. Effects of electrolytic lesion of hypothalamic paraventricular nucleus and its related areas on the sleep waking cycle in the cat. Arch Ital Biol 125:305–315.

Sherin JE, Shiromani PJ, McCarley RW, Saper CB. 1996. Activation of ventrolateral preoptic neurons during sleep. Science 271:216–219.

Shipley MT, Fu L, Ennis M, Liu WL, Aston-Jones G. 1996. Dendrites of locus coeruleus neurons extend preferentially into two pericoerulear zones. J Comp Neurol 365:56–68.

Simpson KL, Altman DW, Wang L, Kirifides ML, Lin RC, Waterhouse BD. 1997. Lateralization and functional organization of the locus coeruleus projection to the trigeminal somatosensory pathway in rat. J Comp Neurol 385:135–147.

Steindler DA. 1981. Locus coeruleus neurons have axons that branch to the forebrain and cerebellum. Brain Res 223:367–373.

Suzuki R, Shimojima H, Funahashi H, Nakajo S, Yamada S, Guan JL, Tsurugano S, Uehara K, Takeyama Y, Kikuyama S, Shioda S. 2002. Orexin-1 receptor immunoreactivity in chemically identified target neurons in the rat hypothalamus. Neurosci Lett 324:5–8.

Swanson LW. 1998. Brain maps: structure of the rat brain. Amsterdam: Elsevier Science Publishers B.V.

Taheri S, Mahmoodi M, Opacka-Juffry J, Ghatei MA, Bloom SR. 1999. Distribution and quantification of immunoreactive orexin A in rat tissues. FEBS Lett 457:157–161.

Thakkar MM, Ramesh V, Strecker RE, McCarley RW. 2001. Microdialysis perfusion of orexin-A in the basal forebrain increases wakefulness in freely behaving rats. Arch Ital Biol 139:313–328.

Thannickal TC, Moore RY, Nienhuis R, Ramanathan L, Gulyani S, Aldrich M, Cornford M, Siegel JM. 2000. Reduced number of hypocretin neurons in human narcolepsy. Neuron 27:469–474.

Valentino RJ, Foote SL, Aston-Jones G. 1983. Corticotropin-releasing fac-

tor activates noradrenergic neurons of the locus coeruleus. Brain Res 270:363–367.

Valentino RJ, Page M, Van Bockstaele E, Aston-Jones G. 1992. Corticotropin-releasing factor innervation of the locus coeruleus region: distribution of fibers and sources of input. Neuroscience 48:689–705.

Valentino RJ, Page ME, Luppi PH, Zhu Y, Van Bockstaele E, Aston-Jones G. 1994. Evidence for widespread afferents to Barrington's nucleus, a brainstem region rich in corticotropin-releasing hormone neurons. Neuroscience 62:125–143.

Valentino RJ, Chen S, Zhu Y, Aston-Jones G. 1996. Evidence for divergent projections to the brain noradrenergic system and the spinal parasympathetic system from Barrington's nucleus. Brain Res 732:1–15.

Van Bockstaele EJ, Colago EE, Valentino RJ. 1996. Corticotropin-releasing factor-containing axon terminals synapse onto catecholamine dendrites and may presynaptically modulate other afferents in the rostral pole of the nucleus locus coeruleus in the rat brain. J Comp Neurol 364:523–534.

Van Bockstaele EJ, Colago EE, Valentino RJ. 1998. Amygdaloid corticotropin-releasing factor targets locus coeruleus dendrites: substrate for the co-ordination of emotional and cognitive limbs of the stress response. J Neuroendocrinol 10:743–757.

Van Bockstaele EJ, Peoples J, Telegan P. 1999a. Efferent projections of the nucleus of the solitary tract to peri-locus coeruleus dendrites in rat brain: evidence for a monosynaptic pathway. J Comp Neurol 412:410–428.

Van Bockstaele EJ, Peoples J, Valentino RJ. 1999b. A.E. Bennett Research Award. Anatomic basis for differential regulation of the rostrolateral peri-locus coeruleus region by limbic afferents. Biol Psychiatry 46: 1352–1363.

Waterhouse BD, Lin CS, Burne RA, Woodward DJ. 1983. The distribution of neocortical projection neurons in the locus coeruleus. J Comp Neurol 217:418–431.